ABSTRACT

Title of Document:	**DESIGN OF A NOVEL PORTABLE FLOW METER FOR MEASUREMENT OF AVERAGE AND PEAK INSPIRATORY FLOW**
	Shaya Jamshidi, M.S., 2009
Directed By:	Professor Dr. Arthur T. Johnson, Fischell Department of Bioengineering

The maximum tolerable physical effort that workers can sustain is of significance across many industrial sectors. These limits can be determined by assessing physiological responses to maximal workloads. Respiratory response is the primary metric to determine energy expenditure in industries that use respirator masks to protect against airborne contaminants. Current studies fail to evaluate endurance under conditions that emulate employee operating environments. Values obtained in artificial laboratory settings may be poor indicators of respiratory performance in actual work environments. To eliminate such discrepancies, equipment that accurately measures peak respiratory flows *in situ* is needed. This study provides a solution in the form of a novel portable flow meter design that accurately measures average and peak inspiratory flow of a user wearing an M40A1 respirator mask.

DESIGN OF A NOVEL PORTABLE FLOW METER FOR MEASUREMENT OF
AVERAGE AND PEAK INSPIRATORY FLOW

By

Shaya Jamshidi

Thesis submitted to the Faculty of the Graduate School of the
University of Maryland, College Park, in partial fulfillment
of the requirements for the degree of
Masters of Science
2009

Advisory Committee:

Professor Dr. Arthur Johnson, Chair

Dr. Adel Shirmohammadi

Dr. Fredrick Wheaton

Acknowledgments

No graduate student can write a thesis by themselves, and this graduate student is no exception. I would like to thank my parents for being the wonderful and selfless people that they are, and moving to two different countries to ensure the very best for their children. I would like to thank my lovely sister, Sarah, who has always been an inspiration in my life, and the best sister I could have ever asked for. I would also like to thank Hamid, my new brother in law, for making me laugh and keeping camp Hamid going. I would also like to thank my cousin Afrooz, for pushing me and adopting me as her little sister.

I would also like to thank my committee members, Dr. Johnson, Dr, Adel and Dr. Wheaton and other professors for giving me guidance when needed and quite frankly – a wonderful education. I have learned a lot from you, and I appreciate every lesson I have learned.

I would like to thank my friends, who are too many to name here, but have made my life so wonderful. I would like to thank Kiri, for going above and beyond to help me and also for enjoying coffee as much as I do. I would like to personally thank my graduate BREGA sisters, Aisha, Melissa and Yin Phan for all of the wonderful times we spent working and learning together. Graduate school would not have been the same without you. I would like to thank Frank, for teaching me many things in the human performance lab. I would like to also thank my college friends, Kolapo, Stacey and Kat, for their encouragement. I would also like to thank Sara for being the very best friend I could have asked for.

I would also like to thank my new coworkers for opening new doors of opportunity to me. My new managers, Susan and Skip, and my coworkers Amber, Audrey, Carey, D.J., Erica, Jack L., Jack Q., Jeff Sa., Jeff Sp., Jeremy, Jerry, Ken, Mark, Robin, Tamara, Tony have made the journey to the "real world" more enjoyable than it should be.

Finally, I would like to thank my lovely Fiancé, Chris, who has brought more joy than I could have every imagined possible. I hope we continue to make each other's dreams come true.

Table of Contents

Acronyms

C2A1	carbon filter canister
ERV	Expiratory Reserve Volume
FP	Fleisch Pneumotachograph
FRC	Functional Residual Capacity
HR_{max}	maximum heart rate
HR_{rest}	resting heart rate
IC	Inspiratory Capacity
IRV	Inspiratory Reserve Volume
M40A1	respirator mask
MFM	mask flow meter
NIOSH	National Institute for Occupational Safety and Health
PC	Personal Computer
PDA	Personal Digital Assistant
PIF	peak inspiratory flow
R^2	coefficient of determination
RV	Residual Volume
SD	standard deviation
TLC	Total Lung Capacity
TV	Tidal Volume
VC	Vital Capacity
VI_{avg}	average inspiratory flow
VO_{2max}	maximal oxygen consumption
VPBS	Variable Profile Breathing Simulator

Chapter 1: Introduction and Justification

The expected maximum daily workloads of employees play an important role in many industries. As the success of a company depends greatly on the productivity of its employees, it is important to understand how the energy requirements of daily tasks affect an employee's work output. To answer this question, one can measure specific physiological response to various work loads. Indeed, the relationships between the physical strain endured by employees and the physical stress applied at discrete work loads lead to the predications and characterizations of productivity that are of interest to management (Maxfield, 1971).

In occupations where employees are exposed to airborne contaminants, the physiological relationship of interest is that between respiratory response and work rate. Flow meters can be used to assess this relationship by measuring ventilation rates and volumes. Moreover, as these occupations typically require the usage of respirator masks to protect the individual from contaminant exposure, flow meters can be used to evaluate the design of respirator masks and carbon filter cartridges. Respirator mask design plays a role in the overall efficacy of human safety programs that mandate their use. Respirator masks may be used as little as 20-30% of the time even when their use in a work environment is compulsory (Harper et al., 1991). They are often rejected due to difficulty in breathing from the added breathing resistance, user discomfort, physiological effects, and the accumulation of sweat inside the mask (Johnson et al., 1997).

The focus of this study is to provide a novel prototype for a flow meter that accurately measures and logs the average inspiratory flow (VI_{avg}) and Peak

Inspiratory Flow (PIF) of subjects wearing a U.S. Army M40A1 respirator mask during exercise. The objectives are to utilize the prototype mask flow meter to measure the maximum tolerable workload of a user wearing a mask, characterize the respiratory health of users, gauge respirator mask comfort, and determine cartridge life cycles.

Previous assessment of these variables were limited to laboratory testing due to non-portable flow meter designs and were insufficient to characterize the respiratory performance of workers *in situ*. Respiratory performance values obtained in artificial laboratory conditions may vary considerably from actual performance in the work environment. The design of an accurate portable flow meter mitigates the difficulty of obtaining representative measurements and facilitates the assessment of personnel respiratory requirements.

Chapter 2: Objectives and Requirements

2-1. Main Objectives

The goal of this research was to provide a means to measure the PIF and VI_{avg} values of a subject wearing a respirator mask (M40A1) and carbon filter canister (C2A1) while exercising. This objective can be divided into three main components, each of which is summarized below.

2-1-1. Flow Meter Design

Design a safe and portable miniature measurement device that accurately measures inspiratory peak and average inhalation values of a subject wearing an M40A1 respirator mask with a C2A1 filter cartridge. The flow meter must not compromise the protection afforded to the user by the filter cartridge nor place the user in undue physical or respiratory stress.

2-1-2. Data Acquisition System

With the aide of a programming language, provide a data acquisition system that obtains and stores flow measurement values. Particular values of interest include VI_{avg} and PIF values. Furthermore, values should be stored in such a manner as to allow data manipulation and statistical analysis. Finally, the system should be designed so that it is easily transportable to field for measurement of real, non-laboratory, values.

2-1-3. Testing

Assess the accuracy of the novel flow measurement device with a breathing simulator, Krug's (Life Science, KRUG International Company; San Antonio, TX) Variable Profile Breathing Simulator (VPBS), used to mimic the natural breathing of

a human. Additional tests will be conducted with human subject at rest and at high work loads.

2-2. System Requirements

With these objectives in mind, a list of system requirements was obtained. This list was used to apply the research objectives to the flow meter system (flow meter, respirator mask and data acquisition system). As such, there are two separate lists of design requirements and design considerations. Design requirements are objectives applied to system components and testing, while design considerations apply to the system as a whole.

2-2-1. Flow Meter Design Requirements

- Measure VI_{avg} at low, moderate and high work loads
- Measure PIF at low, moderate and high work loads
- Maintain measurement disturbance and outside noise at a minimum (high signal to noise ratio)
- Low-voltage requirements – less than 5 volts
- Resistance $\leq$ 3% inhalation resistance of a M40A1 (2.73 cmH2O‧sec/L at 1.42 L/s flow rate)
- Compact Design – approximately 1" in length
- Uphold the safety capabilities of the respirator mask and carbon filter

2-2-2. Data Acquisition System Requirements

- Acquire accurate instantaneous measurements of airflow with a tolerance of $\pm$ 1% for 5 to 600 L/min range
- Store data every 5 minutes
- Support data sampling rate $\geq$ 50 Hz
- Provide operation time $\geq$ 4 hours
- Allow for calibration of the device
- Allow data to be downloaded to a PC
- Permit data manipulation in PC

2-2-3. Experimental Procedure Requirements

- Calibrate the flow meter – steady state and dynamic calibration
- Perform standard operational tasks while performing exercise during experiment

Chapter 3: Literature Overview

The following sections examine results from literature within the context of the study's objectives. The review was divided into three specific subject areas: basic fluid flow concepts, existing flow meter technology, and known human respiratory system characteristics and physiological responses.

3-1. Basic Fluid Flow Concepts

3-1-1. Laminar Flow

At relatively low speeds, when particles of fluid move in straight lines that are parallel to the length of a tube, the flow is considered laminar. Under laminar flow, the Reynolds number is below 2000 and the velocity of the particles in the center of the stream flow is higher than those next to pipe walls. The stream lines remain intact and the velocity profile takes on a parabolic shape. As fluid particles maintain their path of flow, the surface roughness of the pipe is negligible and energy losses are at a minimum. Under laminar conditions, the pressure drop across a pipe is considered directly proportional to the flow. The Hagen-Poiseuille relationship shown in equation 1 can be used to characterize laminar flow (Johnson, 1999).

Equation 1:
$$Q = \frac{Pr^4\pi}{8l\eta}$$

Where: Q = Flow rate
P = Pressure difference along the pipe
r = radius of the pipe
η = viscosity of the fluid
l = pipe length

3-1-2. Turbulent Flow

When fluid particles are highly mixed and the Reynolds number is greatly above 4000, the flow is described as turbulent. Wall friction results in the formation of eddies and vortices in the velocity profile. The rate of energy loss due to friction between fluid particles, referred to as pipe loss, is greatly increased in turbulent flow. Another source of energy loss, referred to as minor losses, is increased due to changes in fluid speed and/or direction. The accumulated loss in fluid energy can be transformed into heat energy, which is then absorbed by the fluid or the environment. In turbulent flow, the pressure drop across the pipe is approximately proportional to the square of the flow (Johnson, 1999).

3-1-3. Transitional Flow

If the Reynolds number is between 2000 and 4000, the flow is neither fully laminar nor fully turbulent. In this type of flow, some signs of turbulence can be seen such as local eddies or vortices. However, these local turbulences are usually reduced further downstream. In this transition zone, calculations of the velocity profile and fluid behavior are non-trivial and may be highly complex (Johnson,1999).

3-2. Flow Meter Design

In determining the most suitable flow design for this project it was necessary to define the parameters of interest. This section describes the selection process employed and examines the technologies of existing flow meters prior to prototype mask flow meter design.

3-2-1. Flow Meter Selection

Currently, there are thousands of flow meters employing various technologies on the market. Choosing the optimal device or technology amidst a vast assortment of competing products requires identification of the design features that would make a flow meter well suited for its intended application. The appropriate flow meter must be able to handle the fluid of interest; in this case, compressible inspiratory air. In addition, the system must be able to be incorporated into the M40A1 mask and C2A1 carbon filter canister for respiratory protective system measurements. This integration should have minimal impact on safety, comfort and ease of use for the user and should not degrade the accuracy of flow measurements. The impact on accuracy can be assessed by computing the expected flow values and then measuring the values produced by each design configuration until an optimal configuration is found for those conditions. Finally, the flow meter must be economically feasible.

3-2-1-1. Selection with Regards to Fluid of Interest

One of the most important considerations in selecting a flow meter is the fluid type to be measured. The limits of detection for flow meters depend on a specific range of fluid properties. Certain flow meters are designed to work optimally with only one fluid type: liquid, gas or vapor. The physical properties of the fluid must be considered. The viscosity, density, temperature and pressure of the fluid can affect how it is handled. The percentage and form of impurities in the fluid of interest are additional factors that must be considered. In some cases, fluids with contaminants must be purified before measurement (Miller, 1983).

3-2-1-2. Selection with Regards to Expectation of Flow Conditions

It is also important to have an expectation of the flow values that are to be measured with the flow meter. The accuracy of flow meters is typically not maintained irrespectively of the range of flow values. Flow meters may need to provide accurate measurements for a single rate of flow, i.e., for a steady state flows; alternatively, they may be used to measure flow of varying rates, i.e., dynamic flow. Dynamic flows require robust measurement devices that produce accurate readings when measuring a wide range of flows.

3-2-1-3. Selection with Regards to Conditions of Installation

The conditions of installation are critical to achieving accurate flow measurements. Of primary concern are the size requirements of the flow meter. Some flow meters have large volumes and cannot be easily scaled down for smaller installation environments. The scaling may also affect the material selection of the flow meter. Some flow meters require upstream flow conditioning with the addition of pipe length to allow for contaminant filtration and removal of turbulent flow effects. It must be noted that while an increase in pipe length may allow for ideal flow conditions, it may also lead to excessive pipe vibrations. Additionally, the environmental conditions of the room or the environment where the measurements are taken are critical (Miller, 1996).

3-2-1-4. Selection with Regards to Economics and Manufacturability

Consideration of the financial implications of designing, manufacturing, and using the flow meter must be examined. Typically such products have initial costs associated with research and development as well as production. Sustainment costs,

i.e., life cycle costs of using the flow meter over an extended time, include maintenance and upgrades and may eventually comprise the bulk of annual costs. These costs include the labor to design the flow meter and the costs of the materials to design a limited quantity. Estimation of cost requires making numerous assumptions about factors including design quality, labor rates, material sources, and overhead. Business cases are used to present these estimated costs and to weigh them against the benefits anticipated to accrue from the use of the flow meter. In some business cases, although the accuracy of the design may warrant a very precise flow measurement system, the cost-benefit ratio may be prohibitively high. If high accuracy and reliability can be obtained with a system that requires minimal upkeep, the flow meter may be a valuable investment (Miller, 1996).

3-2-2. Mass versus Volumetric Flow Meters

Mass flow meters measure the amount of fluid in pounds per hour or kilograms per second. These measurements are not subject to fluctuations due to temperature and pressure oscillations. In contrast, volumetric flow meters are used when the desired fluid measurement is needed in liters per minute or cubic feet per hour. For measurements of volumetric flow rate of a gas, a reference temperature and pressure is needed, as changes in temperature or pressure, affect the gas's kinetic energy and the measured volume. Therefore, these measurements must be specified with reference to the sampling environment's temperature and pressure (Goldstein, 1996). In pulmonary function tests, volumetric flow meters are used and for this reason, only volumetric meters are examined hereafter.

3-2-3. Reduced Cross-Sectional Area Meters

Decreases in pipe diameter in flow meters with a reduced cross-sectional area are compensated by an increase in the fluid velocity as dictated by the principle of conservation of energy. That is, an increase in fluid velocity and consequent increases in kinetic energy will lead to a corresponding decrease in the pressure across the reduced cross-sectional area. The relative simplicity of reduced cross-sectional area flow meters, lack of internal mobile components, and serviceability of external electrical components has led to their widespread usage in various industries (Hayward, 1979). Venturi tubes, orifice and nozzle flow meters are the most common type of reduced cross-sectional area meter and are discussed below.

3-2-3-1. Venturi Tube

The classic Venturi tube can be divided into four sections: cylindrical inlet, convergent entrance, throat and divergent outlet. The cylindrical inlet of the flow meter is specified to be the same size as the air tube diameter, thus permitting seamless integration. The convergent entrance, defined by a gradual decrease in tube diameter, gives rise to an increase in velocity and a decrease in pressure head. The throat has a fixed cross-sectional area in which the velocity will remain constant. Anywhere from six to eight pressure taps are used to estimate the average pressure midway in the throat. The final section of the Venturi tube, the divergent outlet, is characterized by a steady increase in cross-sectional diameter up to the initial pipe diameter. In this case, the velocity is gradually decreased and the pressure increases nearly to the initial inlet pressure. To avoid high loss in pressure, the transitional sections of the Venturi tube must be smooth and have gradual changes. With a cast

iron body and a stainless steel throat, this type of flow meter requires great accuracy and experience in production. Furthermore, a long tube is needed for the full development of flow and increased the accuracy of measurements (Doeblin, 1996). However, a long tube would likely be difficult to integrate within a respirator mask without impacting user comfort and is incompatible with the design specifications for this project.

3-2-3-2. Orifice

An orifice flow meter is a thin plate with a central hole that is perpendicular to the flow. The ratio of the plate thickness to hole diameter, as well as the placement of the hole, can vary depending on the exact type of measurement that is desired. A pressure differential on either side of the plate will allow the user to calculate the volumetric flow rate (Doeblin, 1996). Its ease of construction, low cost, and readily available literature renders it an advantageous flow meter to design.

The simplicity of the orifice, however, does pose several drawbacks. The inherent drawback of this design is that the smoothness of the drilled hole can negatively affect the turbulence of flow. Turbidity cannot be tolerated as it will clog the hole and ultimately cause systemic errors. By the same logic, gases that contain trace amount of liquids require a filtering or heating element to assure accuracy. This is because wear results in the rounding of sharp edges of the hole, leading to inaccurate measurements. Additionally, directly after the plate, eddies are formed and the central flow distribution narrows into a section referred to as the vena contracta. The eddies in the vena contracta cause a large loss in kinetic energy and production of heat, generating a high head loss. Also, due to the inability to measure

the vena contracta, a coefficient of discharge is calculated based on the orifice plate diameter instead. As a result, the coefficient is much lower than 1 and usually ranges around the value of 0.6 implying a reduced effective to free area ratio (Hayward, 1979). The accuracy of the flow meter depends on the scale of pressure difference. The greater the pressure difference, the more accurate the system. Flows that are 30% less than the maximum allowable flow are often inaccurate. Furthermore, the condition of flow that is upstream from the flow meter makes a great difference in the measurement (Doeblin, 1996). For these reasons, this device is not suited to high environmental and mechanical stressors where respirator masks will likely be required.

3-2-3-3. Nozzle

A nozzle flow meter is another variation on the classic orifice plate that allows for smooth and controlled contractions. Due to its streamlined design, the interior surface is more forgiving of harsh abrasive fluids. These flow meters are particularly suited to conditions of high temperature and high velocity (Baker, 1988). Another major advantage to nozzle systems is their relatively high operational accuracy. The accuracy increases as the pressure differential increases; the meter is generally not recommended for use below 10 inches of differential. These advantages, however, are offset by their high cost; the higher the accuracy of the nozzle, the higher the cost. Moreover, installation and cleaning of the interior is often difficult. Therefore, nozzles are almost always used with clean fluids that require little flow meter maintenance. It is not recommended with fluids that build up residue (Hayward, 1979). The low level of accuracy at lower pressure differential combined with the

high costs makes this flow meter an unlikely choice for this project.

3-2-4. Flow Meters Employing Difference in Pressure for Volumetric Measurement

3-2-4-1. Drag Plate

Although drag plate flow meters are not typically thought to be classical differential pressure flow meters, the basic principal behind this flow meter is the use of the difference in pressure to indirectly calculate flow. A drag flow meter contains a drag plate that is circular and placed perpendicular to the flow of the fluid. The plate is hinged to an externally supported cantilevered arm. The plate experiences positive pressure on the upstream face and negative pressure on the downstream face due to small eddies. The plate is then forced to move in the direction of the flow. The arm functions to resist this movement with the aide of a tension wire. Flow measurements are then made with the signal from the tension wire which is proportional to the square of the volumetric flow rate of the fluid. This flow meter does not require an external pressure transducer, as signals from the tension wire are a measure of the pressure difference between the upstream and downstream faces of the drag plate. Another advantage of this flow meter is the low likelihood of sediment buildup due to unobstructed fluid flow along its interior. The flow rate measurement range can also be adjusted with a change in the drag plate surface area. However, a smaller diameter ratio of plate to pipe is needed for greater accuracy, leading to a high head loss. In addition, the plate and hinge arm can support only a limited range of fluid forces with typical diameters up to 100mm (Hayward, 1979). As it cannot be used a wide range of fluid flow rates where accurate, quantitative data is needed, this flow meter does not meet the project design specifications.

Another non-classical differential pressure flow meter is a variable area rotameter. In this flow meter, a circular float is encased within a transparent pipe. Fluid flowing within the pipe causes the float to move from its resting position (a position indicated when the flow is zero) to a particular height. A table can be used to correlate the height of the float to the volumetric fluid flow. The main principle behind the movement of the float is the equilibrium of forces acting on it: the pressure drop across the float corresponds to the forces of gravity of the system and the buoyancy of the float material. Coaxial rotation of the float at a particular height is enabled with surface veins on its body. There are several advantages to this flow meter, where its ease of use is one of the foremost factors. Manufacturability and maintenance of this flow meter is uncomplicated, reducing potential expenditures on repairing and servicing. Indeed, its lack of complicated internal parts allows the flow meter to perform at optimal levels for several years. These advantages come at the expense of inaccuracy, typically at 3% of the reading (Hayward, 1979). This precision is further affected when the flow meter is not stable, and should not be used in applications where vibration and pulsation may occur. In addition, the flow meter only works correctly when it is in the vertical position, as it must have gravity acting on it for it to be in equilibrium. This fact requires design alterations in applications with a horizontal placement (Baker, 1988) and is not applicable for this project. Finally, although visual indications of flow rate may be desired in agricultural and patient biofeedback application, the higher accuracy of digital readouts are more desirable for exercise physiology tests and this application.

Pneumotachographs utilize the concept of fixed orifice flow meter with a variable decrease in pressure due to added resistance. The attainment of laminar flow conditions is attempted with the usage of small diameter tubes. Whereas the pressure differential is directly proportional to the square of the velocity and therefore the square of the volumetric flow rate under turbulent flow, the pressure drop is directly proportional to the flow under laminar flow conditions. For very low flow rates, ranging around 0.5 cm^3/min, the most basic laminar flow meter, a single capillary tube, can be used (Hayward, 1979). This tube is connected to highly responsive micro-manometer. To enable measurement of slightly higher flows, capillaries can be grouped together in a bundle, thus dividing the flow by the number of tubes. Bundles as large as 900 parallel capillary tubes have been built and are in use (Liptak, 1993). In the bundles, some negligible turbulence is experienced at the end of the capillary tubes. This method can be rather expensive. For even higher flows, such as those of approximating peak flow, a honeycomb scheme is used. The honeycomb is typically composed of stacked layers of sheets with a series of triangular cross-sectional areas. There are several advantages to this type of flow meter, the most obvious being the linear flow rate versus pressure relationship over a large range of flows. They require an approximately constant viscosity of fluid; fluctuations in viscosity can upset the linearity of the system. Another major advantage is the stability of internal components; no shifting parts exist. However, these flow meters are typically more expensive and are difficult to clean. Dust and other debris can easily clog the capillary tubes. Over an extended testing regime, the functionality and

accuracy of the system may be substantially impaired by the accumulation of debris and may hinder its use in specific applications (Hayward, 1979).

<u>3-2-4-4. A. Fleisch Pneumotachograph</u>

A particular type of laminar flow meter is the Fleisch Pneumotachograph (FP) designed by Alfred Fleisch that has gained considerable respect in the academic community as an accurate flow meter. A cylindrical tube with a circular cross-section houses the flow meter. This flow meter measures flow in terms of proportional pressure differential measured via ducts across a honeycomb of parallel capillary tubes. The capillary tubes of nearly triangular cross-sections are obtained by rolling a corrugated metal sheet around a central pin of a 1.0mm radius (1981, Zock). Each capillary tube measures to be 0.8 mm in diameter and 32 mm in length. Along the circumference of the flow meter there are two rows of small holes equally distributed in the outer tubes. This design option allows for the flow to be averaged around the circumference of the honeycomb prior to its passage to the pressure measurement ducts. The honeycomb design allows for laminar flow while also acting as a resistance piece. The system's resistance values, equal to or less than 15mm of water, are not expected to hinder the respiratory system. The flow and pressure relationship of the pneumotachographs are linear under capillary flow conditions. When the flow surpasses these conditions, the relationship is no longer linear and deflections in measurement can be observed. In such small tubes, clogging due to the vapor condensations can often cause complications. A circumferential heating element, consuming 6 volts and 1 ampere of electricity, alleviates this problem (1981, Zock).

Currently there are ten models of the FP available on the market. Each model

is specifically designed for linear pressure-flow relationship under certain flow conditions. The diameter, length, dead space, and weight of each model are different. The size of the meter is proportional to its maximum and advisable flow usages. In total, the ten models are used for flows that range from 9ml/s to 25L/s. Undergoing rigorous quality control procedures, each system is provided with calibration values and reference pressure versus flow data points. More specifically, the pressure difference between the two ducts leading to the transducer is related to flow. The barometric pressure can be neglected as this relationship only concerns the flow and air viscosity. Each system is further verified to ensure accurate and equal readings when used for both inhalation and exhalation. Although an interesting prospect, the FP in its current form is not applicable to usage in a portable flow meter where a compact design that can be integrated with the M40A1 and C2A1.

3-2-4-5. Pitot Tube

Pitot tubes are essentially small tubes that act as pressure taps and are perpendicular to the flow of the fluid. Two different values are obtained with pitot tubes: stagnation or total pressure and static pressure of the free flowing stream. The stagnation pressure is the pressure required to convert the kinetic energy of the fluid into pressure. The static pressure is measured by pressure taps on the outside of the pitot tube. The difference between the static pressure and the stagnation pressure is referred to as the dynamic pressure and can be measured by a pressure transducer. The dynamic pressure can be used to evaluate the flow velocity. Typically, pitot tubes are used only to obtain the velocity of the fluid flow in the centre of the tube from the dynamic tap. If several dynamic taps are used, however, the system of tubes

can determine the volume flow rate as an average of the pressure difference in the taps.

The major issue with pitot tubes is the difficulty in attainting accurate measurements. If the tube is misaligned with the velocity profile, the pressure taps may yield readings of a component of the velocity rather than the true value. Thus over a wide range of flow, the accuracy of pitot tubes is generally low and not a great fit for this application (Liptak, 1993).

3-2-5. Rotational Flow Meters

Rotational flow meters contain revolving mechanical components that measure volumetric flow rate of a particular fluid. These flow meters are typically used for liquids. Some alterations must be made for flow meters to be suitable in gas fluid usage. Due to their low density, and therefore low fluid energy, gasses typically lack the energy to propel rotational meters. Therefore, such designs must endeavor to reduce loss of energy. One of the simplest methods to accomplish this goal is to decrease energy lost due to friction. This goal is manifested in various design decisions for the rotational flow meters that are intended for gas measurement. There are two types of meters that are examined: positive displacement root and turbine flow meters.

3-2-5-1. Positive Displacement Root Meters

These flow meters have gears roughly in the shape of the number '8'. It displaces a certain quantity of fluid portioned into volumetric sections and subsequently counts the number of sections that are displaced. It is most accurate in measurement from approximately 15% to 90% of the maximal flow rate. Within this

range where it is most linear, highly accurate measurements of $\pm 0.5\%$ are easily attained (Hayward, 1979). The peak measurement values are $2m^3/s$ with pressure of up to 80bar. As the flow and pressure increases, the weight of the system increases. Thus, these flow meters are rarely used in applications requiring greater than 20bar pressure. Another drawback is the linearity of the pressure versus flow relationship that can become disturbed by upstream flow conditions. The velocity profile is further disturbed with pulsations. Additionally, this flow meter can only tolerate filtered fluids, as any dirt or debris will wear the gear system and reduce tightness of seals and reliability of the readings (Hayward, 1979). With the possibility of reduced seal capabilities and the high probability of pulsations affecting flow measurement, this flow meter is not suited for application in this project.

3-2-5-2. Turbine Flow meters

In this type of flow meter, a rotary fan is used perpendicular to the flow of fluid. The fan is large enough within the pipe to maintain seals with the side walls. The speed at which the fan spins will depend on the flow rate of the fluid. The linear velocity of the fluid determines the rotational velocity of the fan. A sensor is used to determine the rotational velocity of the fan and thus determine the flow rate of the fluid. The blades are either made of magnetic material or have magnetic inserts. A magnetic sensor in the pipe wall measures the speed of the blade crossing a particular point and outputs appropriate voltage values. A digital pulse rate flow meter can measure the instantaneous flow rate. Integrating the pulses with respect to time will attain the total flow of the fluid (Doeblin, 1999). The size of the flow meter affects the speed of blade movement and therefore the volumetric flow rate measurements.

Large flow meters have heavier blades and correspondingly lower flow rates (Hayward, 1979). The turbine's speed is not necessarily linearly proportional with fluid flow rate. By keeping energy losses at a minimum, such as friction and heat buildup, one can aim for a more linear ratio. The effect of viscosity and temperature fluctuations due to friction on the linearity of the meter is most prominent at low flow rates. At higher flow rates, in turbulent flows, the effects of viscosity on linearity of the flow meter are minimal. Manufacturability of a small flow meter is rather difficult, as the geometry and smoothness of the blades and bearing can have significant effects on the velocity profile. Furthermore, there is typically an inertial lag in the response of the fan. Thus for usage in a dynamic system where compact design is required, the turbine flow meter is not a desirable system to use (Doeblin, 1990).

3-3. Human Respiratory System Characteristics and Responses

The prototype mask flow meter is designed to measure the human respiratory system's reaction to assorted workloads. Of primary concern is the ability of the flow meter to correctly capture the complexities of the respiratory cycle during both resting and more dynamic flow conditions of higher work rates. Accordingly, respiratory cycles and volumes as well as average and peak flow rates are examined; in addition, the effects of additional resistance on the respiratory system are considered.

3-3-1. Respiratory Cycles

The respiratory system obtains oxygen and eliminates carbon dioxide by a series of volume and pressure changes in the breathing cycle. This cycle is divided into two phases - inspiration and expiration. The duration of the two phases in the

breathing cycle vary and has been deemed to depend on the workload. At rest, for example, the inhalation portion is approximately one third of the total breathing cycle (Johnson, 2006).

During inspiration, muscles in the thorax work to expand the total volume, decreasing internal pressure and allowing fresh air to rush into the lungs. There are two types of inspiratory modes – quiet and forced inspiration. In quiet inspiration, the diaphragm and intercostal muscles work to increase the thoracic cavity by approximately 500mL. Deep or forced inspiration utilizes additional muscles to further increase the thoracic cavity volume and thus allow a greater volume of gas exchange (Marieb and Hoehn, 2007).

At rest, respiratory muscles relax during expiration, thereby passively compressing the thoracic cavity. This relaxation decreases the thoracic volume and increases the internal pressure, which forces deoxygenated air out of lungs. Forced expiration, on the other hand, can be achieved by actively contracting abdominal wall muscles (Marieb and Hoehn, 2007).

3-3-2. Respiratory Volumes

In pulmonary function tests, several different terms are used to quantify the exact volume of air in the lungs. The four terms used to define respiratory volumes are tidal, inspiratory reserve, expiratory reserve, and residual. These volumes can then be combined to form the four main lung capacities of total lung, vital, inspiratory, and functional residual capacity (Marieb, 2007). These values are given in Table 1.

Table 1. Respiratory Volumes and Capacities (adapted from Marieb, 2007)

Term	Definition	Adult Male Average (mL)	Adult Female Average (mL)
Tidal Volume (TV)	Inhalation and exhalation volume with each breath during rest	500	500
Inspiratory Reserve Volume (IRV)	forced inhalation volume after normal tidal volume inhalation	3100	1900
Expiratory Reserve Volume (ERV)	forced exhalation volume after normal tidal volume exhalation	1200	700
Residual Volume (RV)	Remaining volume of air in lungs after forced exhalation	1200	1100
Total Lung Capacity (TLC)	Max volume of air in lungs after forced inspiration	6000	4200
Vital Capacity (VC)	Max volume of air that can be exhaled after forced inspiration	4800	3100
Inspiratory Capacity (IC)	Max volume of air that can be inspired after normal expiration	3600	2400
Functional Residual Capacity (FRC)	Volume of air in lungs after normal tidal volume exhalation	2400	1800

3-3-3. Average and Peak Inspiratory Flow

Peak flows occur when the flow rate changes rapidly. PIF is defined as the

highest inhalation flow rate achieved over a particular time period.

Typically, PIF values fluctuate around 350 L/min. During exercise, PIF values increase with work rates. More specifically, PIF has been measured by several different laboratories at different levels of VO2 max. At 80% VO2 max, Jansen et al. (2005) obtained 95th percentile peak flow of 365 L/min. At 80 to 85% of VO2 max, Johnson (2006) attained 99th percentile of 359 L/min, with one subject peaking at 442 L/min. At 90%VO2max, peak flow of 321 L/min was found in subjects wearing respiratory protective masks by Berndtssen (2004).

PIF values have been compared to average flow to gain a better understanding of its significance. Specifically, the PIF/ VI_{avg} ratio has been examined in subjects with and without respirator masks during moderate and heavy workloads. This allows researchers to determine the difference between what the subject typically experiences (VI_{avg}) as compared to strenuous conditions (PIF). The ratio depends on the shape of the breathing wave form, with the highest ratio to be expected for a sinusoidal waveform (Johnson, 1991). Peak flow rates can be estimated by multiplying π with average flow rate for sinusoidal wave shapes (Coyne et al., 2006). Jansen et al. (2005) determined values of 2.5 to 3.8 for inhalation only, with a rise in variability with increasing work rate and a decrease in ratio at higher work rates. Moreover, Jansen et al. noted that ratios were typically higher in female subjects than male subjects. Johnson (2005) noted ratios of 2.85 for both sexes during the 50% duty cycle. The assumptions from these methods of determining the peak flow rates are reasonable but not ideal because breathing waveforms at high workloads are similar to trapezoidal or rectangular shapes rather than to sinusoidal forms (Silverman et al.,

1943; La Fortuna et al., 1984; Kaufman and Hastings, 2004).

In subjects with healthy respiratory systems, approximately 1% of all measurements obtained during exercise are PIF values (Johnson, 2006). The relatively short duration of peak flow has allowed some researchers to challenge its significance in measurement. Jansen et al. believe the short duration of PIF and therefore small volume of inhaled unfiltered air render PIF an insignificant metric (Jansen et al., 2005). Coyne et al. (2006), however, assert the significance of PIF by noting that the frequency of occurrence of PIF is not known. If the frequency of PIF occurrence is high, then the volume of inhaled unfiltered air may be high enough to pose a considerable health risk to the user.

Johnson et al. (2006) highlighted yet other reasons for the significance of the measurement of peak flow on filter protection. Johnson's position was that the subject should be an integral part of the mask system. PIF experienced during hard work affects respiratory work, flow wave shape, and developed muscle pressure. Indeed, high PIF can lead to an increase in pressure and thereby an increase in the work rate of the user's respiratory system. These factors, in turn, affect the user's comfort. Based on a survey, subjects who are uncomfortable and have difficulty breathing are more likely to not wear masks, regardless of hazardous conditions. Therefore, human needs cannot be dismissed in favor of practicality in mask design. Furthermore, designing a flow meter that accurately measures the peak flow is imperative in mask design and respiratory research (Johnson, 2006).

An ideal instrument is one that not only measures the normal values, but also the minimum and maximum values as well. In the case of flow meters, the maximum

value corresponds to the peak flow. As such, it follows that peak flows should inherently be measured to give users the full range of values experienced during work.

3-3-4. Inspiratory Resistance

The effect of resistance on work performance is a critical factor that must be considered in respiratory protective systems. Drastic decrease in work time and misuse or lack of usage of the respirator masks are among the negative consequences associated with the high resistance values.

Johnson et al. (1999) tested six men and women between the ages of 18 to 34 with an M17 full face piece mask. Each subject was tested with six discrete resistance levels at a flow rate of 85L/m at 80 to 85% of their VO2 max. At a very high level of significance, they observed that performance time decreased linearly as resistance level increased.

When the resistance is increased, the inhalation flow characteristics change from laminar to more turbulent flow. With this change, the percentage of expiration in the breath cycle is reduced. Furthermore, as the exhalation percentage decreases due to an increase in work load, the total work time decreases. Ultimately, any increase in inspiratory resistance leads to turbulent inspiratory flow, a decrease in the percentage of expiration, and a decrease in work performance (Johnson et al., 1973).

Inspiratory resistance must be translated into design goals, by aiming to maintain as low a total resistance value as feasible. The respirator mask and carbon filter cartridge alone, with a resistance level of approximately 2.73 cmH2O.sec/L, accounts for a 25% decrease in performance (Johnson, 1999). Any great addition to

resistance will greatly hinder workers and is undesirable.

The design goal of decreasing resistance as safely as possible has been argued by Deno et al. (1981) and Babb et al. (1989), who were unable to properly test the relationship between inspiratory resistance and work performance. They concluded that inspiratory resistance has minimal to no significant effect on performance times. This conclusion, however, cannot be upheld in a general context as subjects were tested outside of work rate that would induce respiratory stress, the respiratory sensitivity range. When the performance time ranges from five to fifteen minutes, the work is most sensitive to respiratory stress. Relatively higher workloads are sensitive to cardiovascular stress, while lower ones are sensitive to thermal stress (Johnson and Cummings, 1975). Therefore, unless subjects are under work loads that approach 80-85% of their VO2 max, they will note little variation in their overall work function due to increase in inspiratory resistance (Caretti et al.,1998).

Chapter 4: Methods

The methods of this project can be divided into two main components, each of which is targeted toward the realization of the previously discussed objectives (chapter 2). Methods detailing the system development, including final Mask Flow Meter (MFM) design and data acquisition system, in addition to experimental tests which verified the accuracy of the MFM system are presented in this section.

4-1. System Development

4-1-1. Flow Meter Design

The final MFM design was a pressure differential meter with a wire mesh screen used as the resistance piece for a compact design (engineering drawings in Appendix A).

Implementation of a compact design was made possible through the employment of two aluminum mesh screens adhered together to form the resistive element in the MFM. The usage of the two mesh screens was derived after several iterative tests indicated their specific advantage in maintaining resistance small enough to not hinder the natural breathing cycle while at the same time producing a pressure difference detectable by the pressure transducer (results in section 4-1-1-1).

Ports were used to allow for the attachment of a pressure transducer (5 INCH D-4V, manufactured by All sensors, Morgan Hill, CA) to the main body of MFM. The inlets to the pressure transducer were positioned such that one inlet was placed on either side of the mesh screen to measure the pressure difference across the screen.

A modular design was chosen so that all internal components can be easily replaced and or upgraded, thus easing any needed maintenance (Figure 1). There are

six internal components: 2 inner tubes, 1 mesh mounting ring, 1 mesh resistance, 1 mesh locking ring, and 1 gasket. Two inner tubes are used as spacers for the pressure transducer ports. With four small holes placed along the circumference of the inner tubes, an average of the flow was obtained by the pressure transducer. The mesh resistance piece was held in place with a mesh mounting and locking ring. Finally, a single gasket was used to ensure tight seals. As the respirator mask is fitted with its own rubber gasket, an additional gasket is not required for the MFM – respirator mask connection.

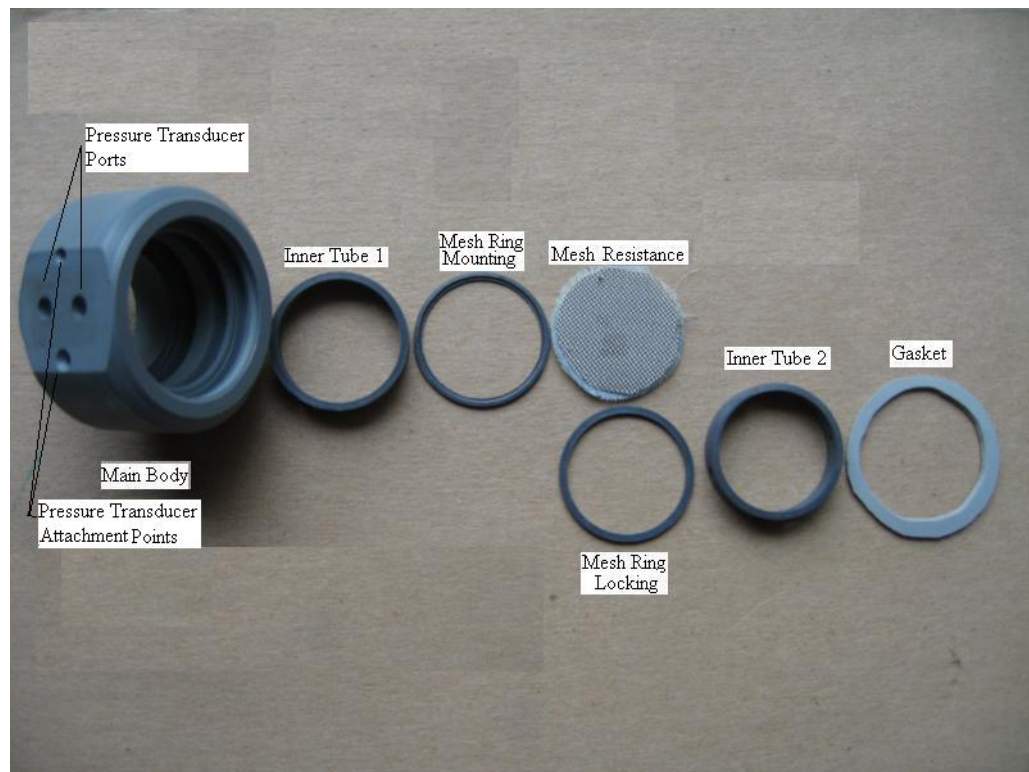Figure 1. Final form of Prototype Mask Flow Meter with Seven Components

For the simplest design, the MFM should be external to the mask and connected to one of the M40A1 respirator mask inhalation outlets. In this way, there is no need for additional cutouts or alterations to the respirator mask and the flow of inhaled air must pass through the MFM. Two locations were identified that met these

conditions: outside the C2A1 filter canister or between the canister and the respirator mask. Concerns about measuring laminar flow with a screen were addressed by placing the flow meter in between the C2A1 filter canister and the M40A1 respirator mask. In this way, the reduced diameter of the channel flow due to the carbon particles embedded in the C2A1 can reduce the presence of eddies and vortices and therefore decrease the Reynolds number. An additional advantage of this placement is the low probability of having the mesh screen clogged as the C2A1 will filter debris and particulates.

In the final design, the MFM body was connected to both the respirator mask and carbon filter canister with unique National Institute for Occupational Safety and Health (NIOSH) threads (Appendix A). On the side connecting the MFM to the mask, male threads were utilized. The filter side of the MFM required female threads. Determination of the number of threads presented an issue as it affects the stability of the flow meter. On the one hand, a high number of threads decreases the probability that the MFM will loosen during operations where the mask and carbon filter canister are subject to the highest stress loads. Numerous threads, on the other hand, unnecessarily elongate the body of the flow meter and add excessive torque to the mask. Therefore, the smallest number of threads that would allow for a stable system was determined. This number was derived from observations of C2A1 carbon filter canister connection to the M40. When attaching the C2A1 carbon filter canister to the M40, only two full threads are used. As stability of the carbon filter canister and respirator mask combination has been demonstrated by its years of usage, the same number of threads was chosen for the MFM.

Another direct advantage to a compact design is a decrease in the overall weight of the MFM. The weight of the MFM must be kept to a minimum to avoid a large increase in weight to respiratory protective equipment worn by users. Although the thick straps act as the suspension system for the respirator mask and hold the canister when the wearer is stationary, when the wearer is running the weight of the carbon filter canister causes it to jump and pull on the wearer's head. Furthermore, when worn for long periods of time, the friction caused by straps rubbing on the wearer's head could result in sensitivity around the metal buckles. Friction of the nose cup and jerky movements of the mask can lead to discomfort and even pain for wearers. For these reasons, it was imperative that the MFM adhere to a compact size and light weight.

4-1-1-1. Screen Mesh Resistance Determination

Meshes with a wide range of porosity values were individually inserted into a tube of a six inch length. The material of the tube was consistent with the material of the prototype (polyvinyl chloride) as to alleviate material frictional differences that could lead to pipe loss. The tube was then attached to a steady state flow source and the pressure difference was obtained at low flow values with a pressure transducer. In addition, the tube alone was connected to a breathing simulator device to serve as a control. The final mesh resistance choice was one with the least resistance needed for a pressure difference measured by the pressure transducer.

Four varieties of mesh screens were iteratively used to determine the type for which the optimal balance between the tolerated resistance and pressure differential could be achieved. At a steady flow of approximately 50 L/min, the voltage output

30

and pressure equivalent of a single pressure transducer were measured for each screen

(Table 2).

Table 2. Voltage and Pressure Output from Pressure Transducer in Response to Various Mesh Resistance Values

Mesh Screen Description	Pressure Transducer Output (V)	Pressure Equivalent (cmH2O)
Control	1.4	-5.43198
High Porosity Fabric Screen – Nylon	1.44	-5.191608
High Porosity Fabric Screen – Cotton	1.45	-5.131515
Stainless Steel Screen*	2.01	-1.766307
2 Stainless Steel Screens*	2.98	4.062714

Note: Stainless Steel Screens were made of 16 wires per inch, with 0.018 inch wire diameter.

The control was measured without a screen and represents the pressure transducer output with zero resistance. Note that 0 V is not equal to 0 cmH2O pressure. The negative pressure value is as a result of the operating pressure of the pressure transducer which ranges nominally from $\pm$ 5 V. The fabric screens with high porosity had pressure drop values across the materials that were very similar to that of the control. In these cases, there is essentially no resistance afforded by the screens that can allow the pressure transducer to detect a pressure difference from its two pressure ports. The fabric screens were therefore rejected for usage in the final MFM. An improvement in the ability to detect a pressure difference is seen with the use of a single stainless steel screen mesh. The voltage output of one screen, however, was too low and therefore deemed inadequate. In the next iteration, two screens were sewn together with stainless steel threads and was the first treatment that produced a

viable, non-negative pressure output result. To test the upper limit of detection, the final treatment of low porosity polyester was used and resulted in excessive resistance. It should be noted here that the alignment of the stainless steel threads of the two screens is crucial to avoiding turbulence. Since the process of achieving sewing the two screens is not a manufacturing process, care can be taken to achieve a nearly perfect overlap of the two screens.

From the iterative mesh resistance experiment, the results indicated that the combination of two mesh screens yielded the lowest resistance that was detectable by the pressure transducer. Two stainless screens were used in the final MFM design due to their low but detectable resistance. The use of stainless steel screens has an additional hygiene advantage as it can be cleaned between uses. Additionally, when compared to cloth screens, stainless steel does not absorb moisture and therefore does not affect the resistance.

4-1-1-2. Variability in Pressure Transducers

There are two different pressure transducers (specifications in Appendix E) that were used in experiments; one connected to the FP and deemed the true voltage and the other connected to the MFM. It was necessary to verify the voltage output of the two pressure transducers was equivalent for a given flow. Large differences in the outputs of the pressure transducers could result in systematic errors in flow measurement.

A comparison of the voltage output from the two pressure transducers (Figure 2) combined with the t-test results in Table 2, reveals a statistically insignificant difference between the two pressure transducers. Therefore, systematic errors due to

the pressure transducer output variability were considered negligible.
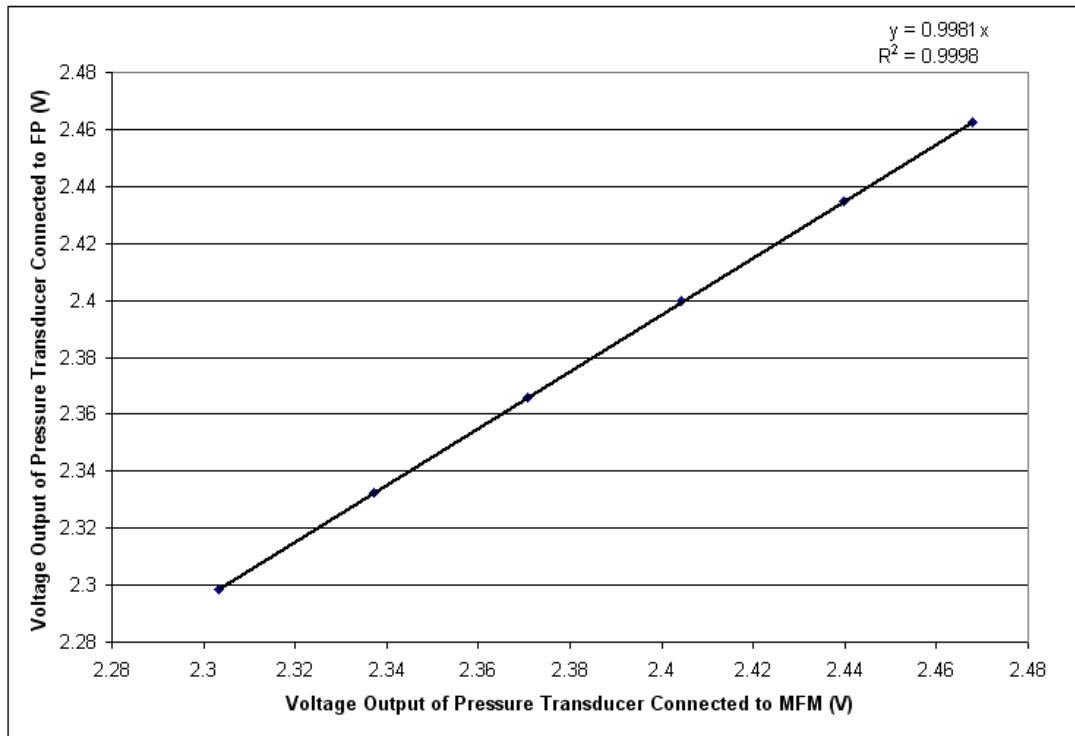
Figure 2. Voltage Output Comparison of the Pressure Transducers Connected to the MFM and FP

Table 3. T-Test Results from Two Pressure Transducers Used in the FP and MFM Systems

t-Test: Two-Sample Assuming Unequal Variances		
	Pressure Transducer for MFM	Pressure Transducer for FP
Mean	2.38707	2.38229
Variance	0.00387	0.00386
P(T<=t) two-tail	0.89684	
t Critical two-tail	2.22814	

4-1-2. Data Acquisition

A military grade pressure transducer (5-inch-d-4v manufactured by All Sensors, Morgan Hill, CA) used in conjunction with the MFM will output a voltage due to the measured pressure difference across the mesh screen. This voltage must be converted to a flow value in order for the system to be of use as a portable flow meter.

The conversion of pressure transducer (specification in Appendix E) voltage output to measured flow occurs through a series of steps (Figure 3). In the first step, the output of the pressure transducer is sent to a data acquisition card. In the second step, an external data acquisition card, USB6009 (specifications in Appendix F) acquires the voltage at 12 bits and outputs processed data in the form of an analog signal at 12 bits. A third step, occurring with the aide of a computer program developed in LabVIEW 7.1 (National Instruments, Austin, TX), converts the voltage data to flow data (Appendix D).
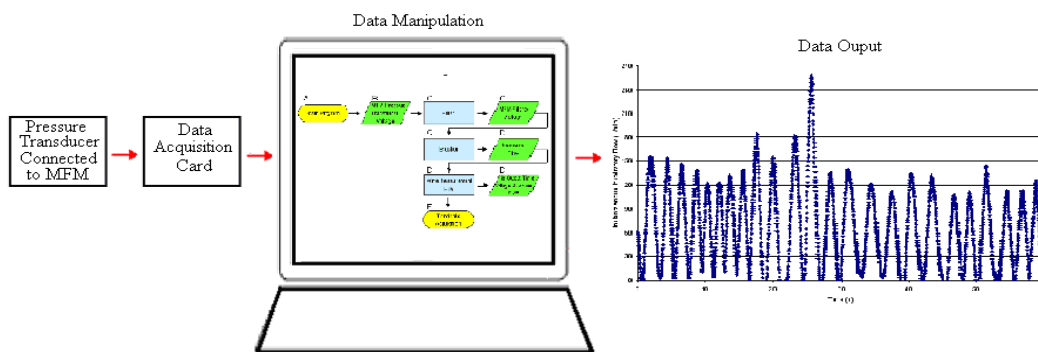
Figure 3. Schematic of Information from the Pressure Transducer to Flow Output

The National Instrument's USB6009 is a full speed universal serial bus interface with eight analog inputs, two analog outputs and 12 ports for digital input or output. In additional to the ports in the USB6009 for data acquisition, there are also two ports for powering external devices (+ 2.5V and +5 V) as well as 12 ports for grounding. The particular ports and channels of USB6009 are displayed in Appendix F. As the pressure transducer has an analog output, only the analog ports in the USB6009 were needed. However, as the system is portable, the pressure transducer was also powered and grounded with the USB6009. Specifically, the pressure transducer requires 3.5 V and therefore the +5V port of USB6009 was used. The pressure transducer was connected via three wires to four ports in the USB6009. A schematic of the pressure transducer pin connections is shown in Figure 4. The pressure transducer was connected to the analogue inputs of the USB6009 at 12 bits. The sampling accuracy of the USB6009, and therefore the system overall, is at 2^{-12}, or 0.00024414. For this reason, all measurements can be made safely at an accuracy of 0.001.
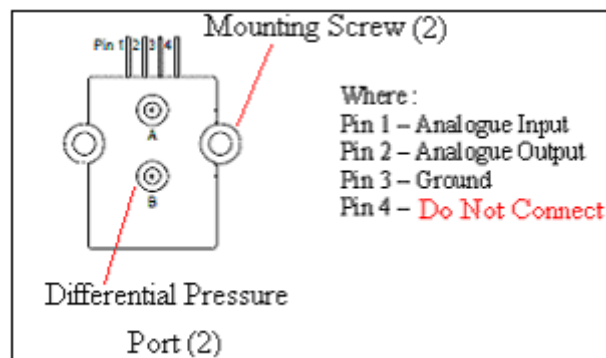
Figure 4. Pin Layout of Pressure Transducer

The virtual instrument (VI) was created with LabVIEW which utilizes various icons within the block diagram of the program. The final version of the program's block diagram and user interface are available in Appendix D. The program is composed of five main phases: (A) initiation, (B) data acquisition, (C) data manipulation, (D) data output, and (E) termination. Figure 5 depicts the manipulation of the data within the virtual instrument program and highlights the phases.
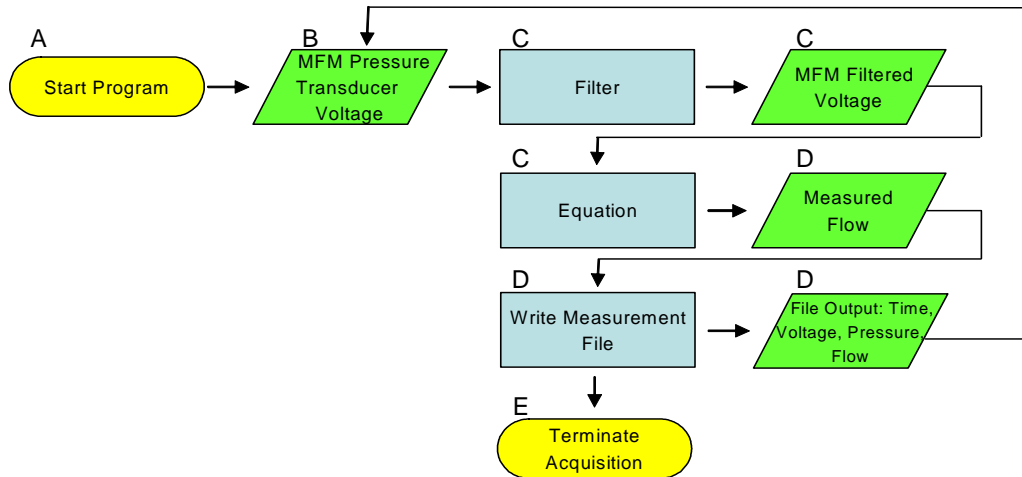
Figure 5. Program Data Manipulation Process

Note: Program will run continuously unless terminated by user.

The data manipulation process occurred by a series of sub-components within the program that converted voltage input to measured flow output. Figure 6 illustrates the operational sequence, user inputs and program outputs of each sub-component in the virtual instrument program. Note the individual processes in the block diagrams are labeled to indicate the particular phase goals they accomplish.

36
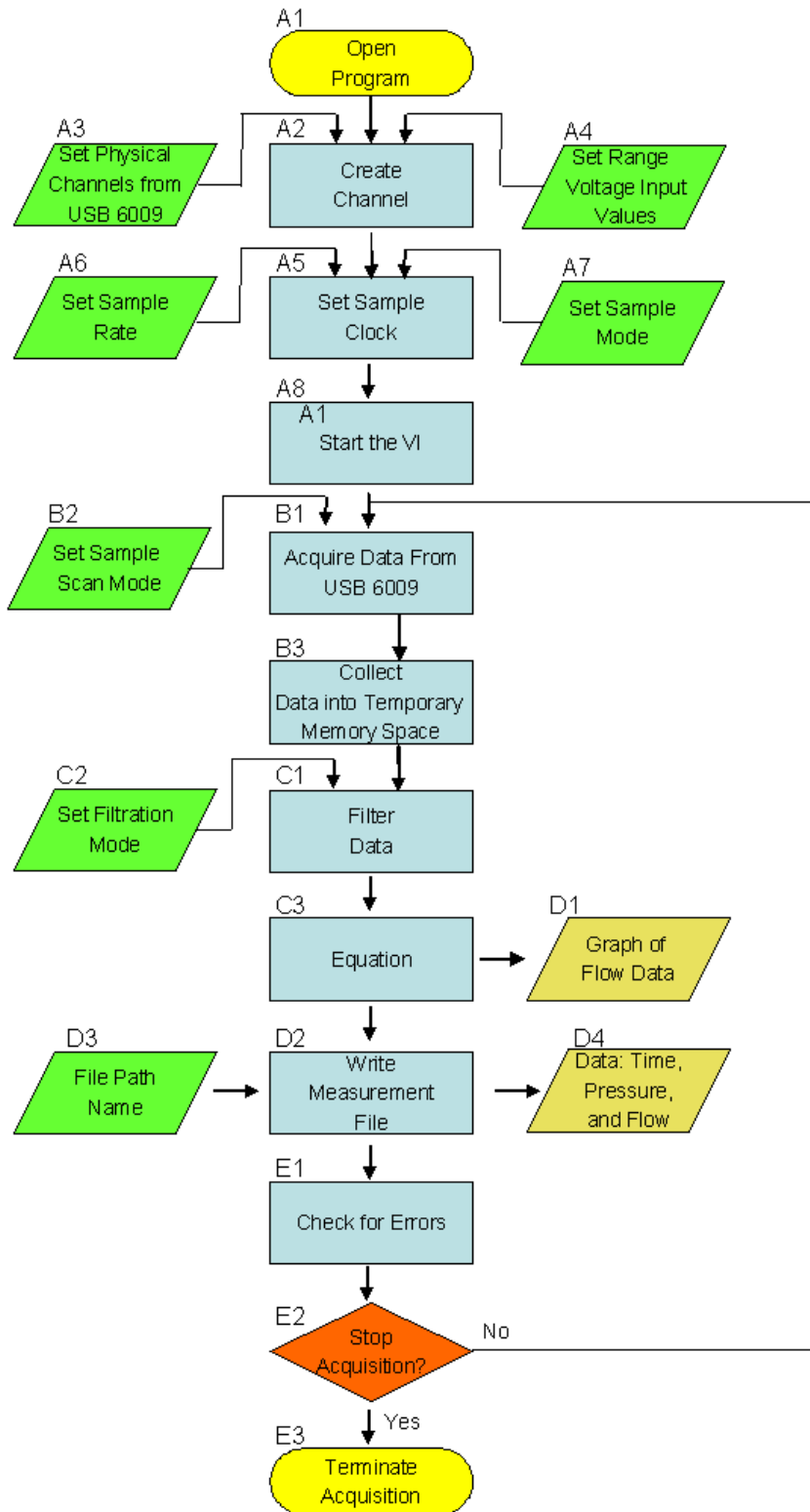
Figure 6. Program Operational Sequence Diagram

Note: Program will run continuously unless terminated by user.

4-1-2-2-1. Program Initiation

The program can be initiated by the user opening the program file and a simple click of the run icon (Block A1).

4-1-2-2-2. DAQmx Create Channel (AI – Voltage BASIC).VI

This particular sub-component (Block A2) connects the USB6009 ports used by the pressure transducer to those that are called in the program. The user specified physical channel inputs and outputs in this sub-component acquire the raw data from the USB6009 (Block A3). In addition, the user can specify the maximum and minimum expected voltage values and thus increase the system's sensitivity to voltage changes (Block A4).

4-1-2-2-3. DAQmx Timing (Sample Clock).VI

This sub-component (Block A5) is used to set the sampling rate and particular mode of acquiring samples. As specified in the objective (Chapter 2), the sampling rate is 50Hz (Block A6). Another input to the sample clock is the sample modes (Block A7). In finite sample mode, the user will specify a number of samples to be acquired. This particular mode is typically used for systems that are characteristically static, where a particular number of samples is needed for statistical evaluation. The sample mode was set to continuous as other sample modes will lead to gaps in the data acquisition and therefore a misrepresentation of the dynamic human respiratory system.

4-1-2-2-4. DAQmx Start Task.VI

This sub-component (Block A8) is needed to assign a task name for internal

processing code used within LabVIEW. This is a precursor step to data acquisition. A task name is assigned to each run of the program with this particular sub-component. The program will not run without a specified task.

4-1-2-2-5. DAQmx Read (Analog 1-D wfm Nchan Nsample).VI

This sub-component (Block B1) reads the data and requires several user inputs. The first user input (Block B2) is the samples taken or the number of samples per input channel. Not to be confused with the finite number of samples, this input specifies the number of samples that the program will 'scan' into the buffer. The input is set to -1 to dictate collection of all the data simultaneously as opposed to sequentially. This greatly increases the speed of sample collection. Moreover, in cases where samples will be acquired for long durations, the speed of sample collection will decrease if this input is not set to -1.

4-1-2-2-6. Collector.VI

Under normal circumstances, the virtual instrument program will take the data and manipulate and store each instantaneous data point individually. This is a useful option if the individual does not need to visualize the raw data as it is being acquired. The collector (Block B3) is used as a temporary storage allowing the individual to see all the acquired data in the graphs.

4-1-2-2-7. Filter.VI

A filter (Block C1) is needed to decrease the noise and therefore to increase the signal to noise ratio for accurate readings. The filter specified in this program (Block C2) is a Butterworth filter with a slow rolloff between the passband and stopband frequencies, producing a smooth response at all frequencies. The specified

cut off frequency is set internally by National Instruments to correlated with the sampling rate. With the aide of this filter, harsh spikes in raw data typically caused by noise are dampened.

To avoid aliasing the data, there are options of filtering out the noise externally with a simple low pass resistor capacitor circuit with a cutoff frequency of 25 Hz. For this specific case, however, it is best to perform this task internally within the program and therefore decrease the number of external components that could potentially decrease the lifecycle of the system as a whole. Ultimately, this decreases the likelihood of damage to the system from a harsh external environment. This option was chosen because the number of samples sufficiently depicted the sinusoidal waves of the VPBS specified at 30 breaths per minute. Higher frequencies at 45 breaths per minute were also tested, and again, the data were displayed correctly.

4-1-2-2-8. Equation.VI

The equation (Block C3) used converted the collected filtered voltage output from MFM's pressure transducer into measured flow. The equation is presented in section 5-1. The equation was derived from the results of a series of transformative steps and calibration procedures. Details of procedures of the transformative and calibration steps are discussed in section 5-1. A graphical output of instantaneous flow versus time is presented to the user on the front panel (Block D1).

4-1-2-2-9. Write LabVIEW Measurement File.VI

The different outputs (voltage, pressure and flow) are collected in a signal merger and transferred to a Write LabVIEW Measurement File sub-component (Block D2). The merger allows for the data to be consolidated and displayed in

separate columns of an Excel file. There are several inputs to this sub-component, only two of which were deemed necessary. The first is the file name (Block D3) that allows the user to specify the file name and the particular location where the file will be saved. The format should be similar to *C:\voltage_file\ run1.lvm* where the file is called "run1" and is saved in the "voltage_file" folder. It should be noted here that LabVIEW does not properly process spaces and punctuation marks. Therefore, the file name and location should be only in the format shown. An added advantage of using numerical values after the file name such as "run1" is the automated ability of the virtual instrument program to save additional files sequentially. There are no limits to the numbers and multiple digits can be used. New files are saved under the same name with an increase in the previous filename's number, ie., "run2".

An additional input is the "OK" to write all virtual button (Block D4). This button is a binary true or false input button that can be pressed by the user in the front panel to logically control whether all data is written to the file or not. The default condition of this button is false and only when it is pressed will there be a switch to a true condition. Under the true condition, all the data that is stored in the buffer will be written to a file at the sample rate specified in the Sample Clock.VI of 50Hz. This input is useful in testing situations where the user can first determine whether the data should be written to a file and subsequently press the button and generate a file with a complete set of acquired data.

Once the user inputs are made, the output of Write LabVIEW Measurement File.VI is an Excel file (D5) with four columns of time, voltage, pressure and flow outputs.

4-1-2-2-10. Simple Error Handler.VI

This sub-component (E1) is one of the most important in the program as it determines whether a programmatic error has occurred. When an error has occurred, this sub-component displays the error and provides guidance for correcting it. The complete list of errors is set by National Instruments and is inherent in the source code of the LabVIEW 7.1 program.

4-1-2-2-11. Terminate Acquisition Button

The program can be terminated by the user (Block E2) by depressing a virtual stop button on the front panel. This button is a binary true or false input button.   The default condition of this button is off (false condition) and only when it is pressed will there be a switch to an on position (true condition). In the on position, the program will terminate.

4-1-2-2-12. Clear Task.VI

This sub-component (Block E3) is required to work in conjunction with the Create_Task.VI sub-component so that it can clear the task that was previously created. Once the task is cleared, the program will terminate automatically.

4-1-3 Preliminary Data Acquisition Results

The development of the MFM system was an iterative design process that required the results from one method for the refinement of the proceeding step. The preliminary methods and results utilized for the development of the MFM hardware and software components are discussed in the following sections.

The data acquisition system used in this study converted the voltage output of the pressure transducer connected to the MFM to measured flow values.   A

preliminary attempt at accomplishing this goal was made with a Personal Digital Assistant (PDA) and LabVIEW PDA module. Initial design incorporated a PDA that would enable the user to easily transport the data acquisition system and provide the same computing and storage capabilities of a computer. At the time of conception, the state of PDA technology commercially available and the novelty of the LabVIEW PDA module made this attempt unproductive. At the time, LabVIEW PDA module was new on the market and had numerous documented issues including software requirements, software tools required, supported devices, creating and sharing variables, exportation of data from PDA to the computer and overall program errors requiring several versions and their updates. When the program was implemented on the PDA, the program was often automatically aborted due to either LabVIEW module source code or PDA processing issues. Given the requirements of this study, where a minimum operational time of four hours was required, this system was not reliable and therefore abandoned.

The present technology of small, portable laptops has presented itself as a superior option for a portable flow meter system. By meeting the requirements specified in Table 4, any small portable laptop can be used. It should be noted that the laptop can be smaller laptops, or mini notebooks, such as the Dell Mini 12. With the addition of memory and Windows XP operating system, this mini notebook can perform at the same level as a laptop and weighs only three pounds.

Table 4. Minimum Requirements for MFM Computing System

System Characteristic	Minimum Specifications Requirement
Processor Speed	1.3 GHz
Operating System	Windows XP
Memory	8 GB
Hard Drive	40 GB, 5400 RPM
Battery Option	24WHr Lithium-Ion Battery
External Connections	USB

4-1-3-1. Preliminary Program Development Results:

The overarching equation used in the program described above was derived from a series of subordinate steps. As the accuracy of this equation depends heavily on these subordinate steps, a series of experiments were utilized to assure the accuracy and precision of each step.   The subordinate steps were used in the computation of measured flow rate from voltage output of the pressure transducer. The accuracy of these steps was assessed with comparative analysis of measured and true values.   The true values in all experiments were provided by the FP and the pressure transducer connected to the FP. One comparative analysis evaluated the raw voltage of the MFM to voltage (section 4-1-3-1-1). A second analysis was used to transform the measured voltage into pressure (section 4-1-3-1-2).   Finally, the measured pressure values of the MFM were compared with flow (section 4-1-3-1-3).

4-1-3-1-1. Raw Measured Voltage to Voltage Comparison

A setup shown in Figure 7 compared the voltage readings from the pressure transducers connected to the MFM and true voltage provided by pressure transducer

connected to the FP.   A steady state flow source was used when recording the
pressure transducers' outputs to a 26 flow levels from zero to approximately 400
L/min. This was possible by acute changes in the valve position of the steady state
flow source. At each flow level, readings were taken for 30 seconds constituting one
trial. Furthermore, three trials were taken at each flow level.

The measured voltage values were compared to true voltage, and an equation
was derived to relate the two voltages. Consequently, the voltage readings from the
MFM were fit to a nearly linear equation.
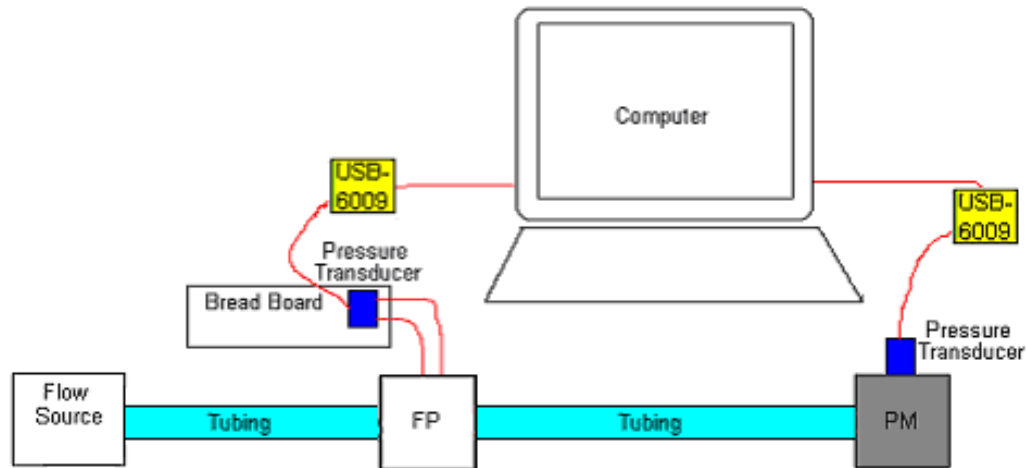
Figure7. Setup for steady state measurement of flow comparing FP to MFM

A total of 4500 data points for each flow level and a total of 117,000 data
points in total were collected for this procedure. To reduce the data points to a more
manageable format and make the system more statistically robust, only the mean
values for each flow level were considered. Finally, an average of each trial result
was taken and used for analysis. In this way, only the means of the means were
considered. The results for this process are summarized in Table 5. The methodology
for this process resulted in a series of experimental errors. Initially, the outputs from

the pressure transducers were used as indicator of the flow value. Changes in flow level, however, were observed to be on the order of 10^{-3} voltage output, including substantial variation in the flow levels of the trials.

Table 5. MFM Measured Voltage to Voltage Comparison

Flow Level	MFM Measured Voltage (V)	True Voltage (V)
0	2.282	2.291
1	2.285	2.296
2	2.290	2.301
3	2.296	2.307
4	2.302	2.314
5	2.313	2.319
6	2.328	2.332
7	**2.348**	**2.343**
8	2.366	2.351
9	2.376	2.356
10	2.385	2.356
11	2.402	2.367
12	2.405	2.364
13	2.435	2.373
14	2.449	2.383
15	2.469	2.386
16	2.484	2.400
17	2.491	2.402
18	2.509	2.403
19	2.523	2.406
20	2.542	2.412
21	2.555	2.416
22	2.581	2.423
23	2.603	2.429
24	2.627	2.436
25	2.635	2.437
26	2.646	2.437

To examine this relationship further, the pressure transducer outputs of the FP and MFM were plotted against each other (Figure 8). Although it was expected that a linear regression would best characterize this relationship, polynomial curve-fitting was performed (Figure 9).
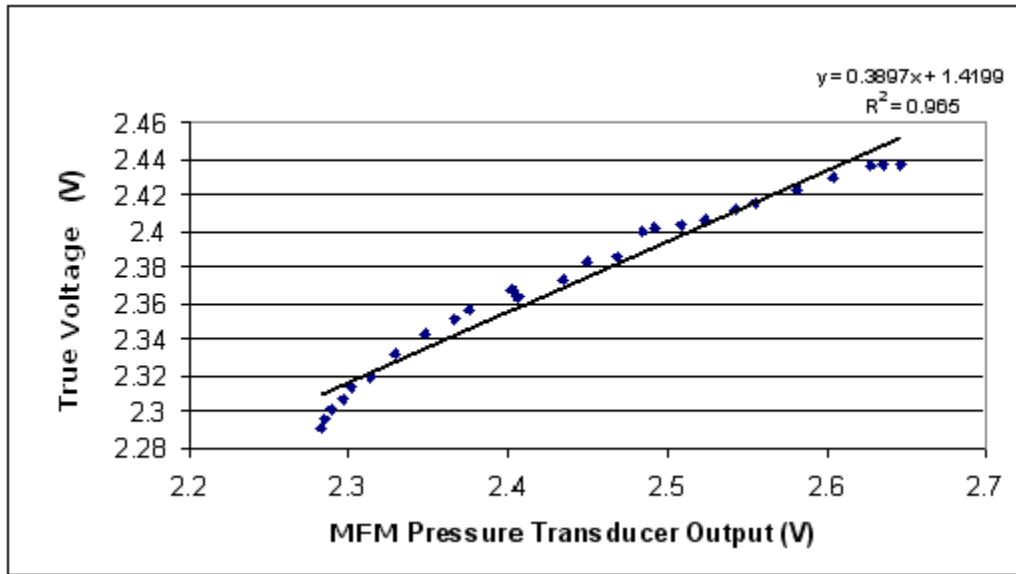
Figure 8. MFM Measured Voltage Compared to True (FP) Voltage at 26 Flow Levels from a Continuous Flow Source – Linear Relationship Examined
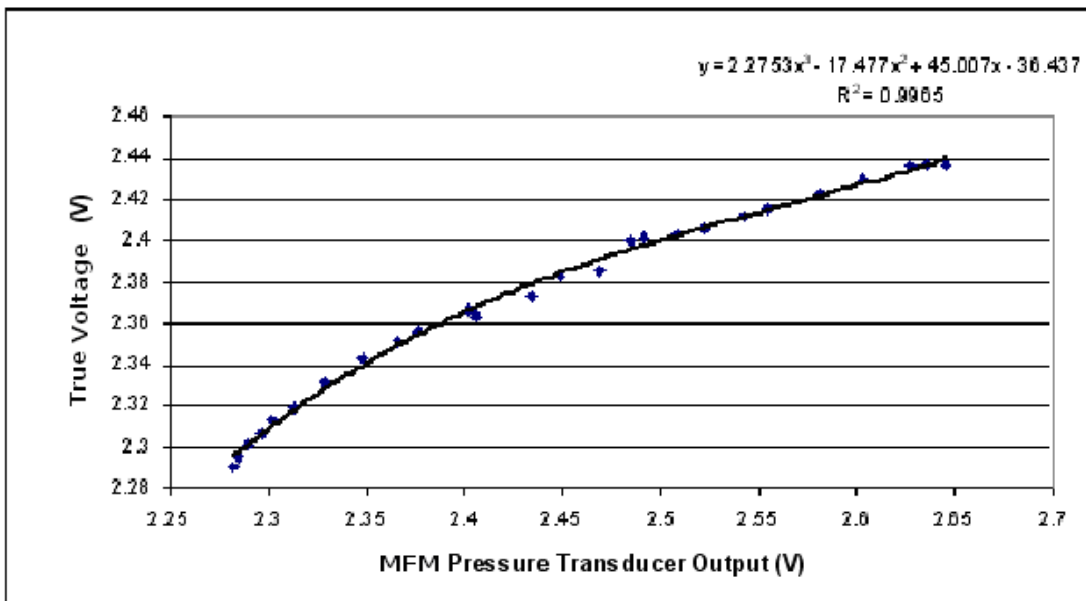
Figure 9. MFM Measured Voltage Compared to True (FP) Voltage at 26 Flow Levels from a Continuous Flow Source – Polynomial Relationship Examined

As Figure 9 demonstrates, a polynomial model best describes the relationship at low and high flows. A higher coefficient of determination ($R^2 = 0.9965$) was observed with the polynomial model. From the results of this experiment, the formula used in the MFM program was a third-order polynomial (equation 2).

Equation 2: $Y = 2.2753X^3 - 17.477X^2 + 45.007X - 36.437$

Where: X = voltage from the MFM pressure transducer (V)
Y = True Voltage (V)

4-1-3-1-2. Measured Voltage to Pressure Comparison

A second equation was used to compare the output voltage readings from the pressure transducers to input pressure values in cmH2O. A syringe, connected to an inlet port of the pressure transducer, was used to inject air at different pressures into the pressure transducer. A manometer was used to monitor actual input pressure. The MFM pressure transducer was calibrated for 0, 0.2, 0.4, 0.6, 0.8 and 1 cmH2O of pressure and the pressure-voltage relationship was obtained. Three separate samples were taken for each of the six treatments with pressures ranging from 0 to 1 cmH2O pressure (Table 6, as well as Figures 9 and 10). The low standard deviation indicated very low variability in the samples of each treatment.

Table 6. Voltage Output from a Single Pressure Transducer due to Applied Pressure
Measured with Manometer

| Applied Pressure (cmH2O) | Outputs from Pressure Transducer | | | | |
	Trial 1 (V)	Trial 2 (V)	Trial 3 (V)	Average (V)	Standard Deviation (V)
0	2.299	2.303	2.309	2.303	0.005
0.2	2.337	2.343	2.3309	2.337	0.006
0.4	2.374	2.375	2.361	2.370	0.008
0.6	2.413	2.405	2.395	2.404	0.009
0.8	2.445	2.438	2.435	2.440	0.005
1	2.475	2.471	2.457	2.468	0.010
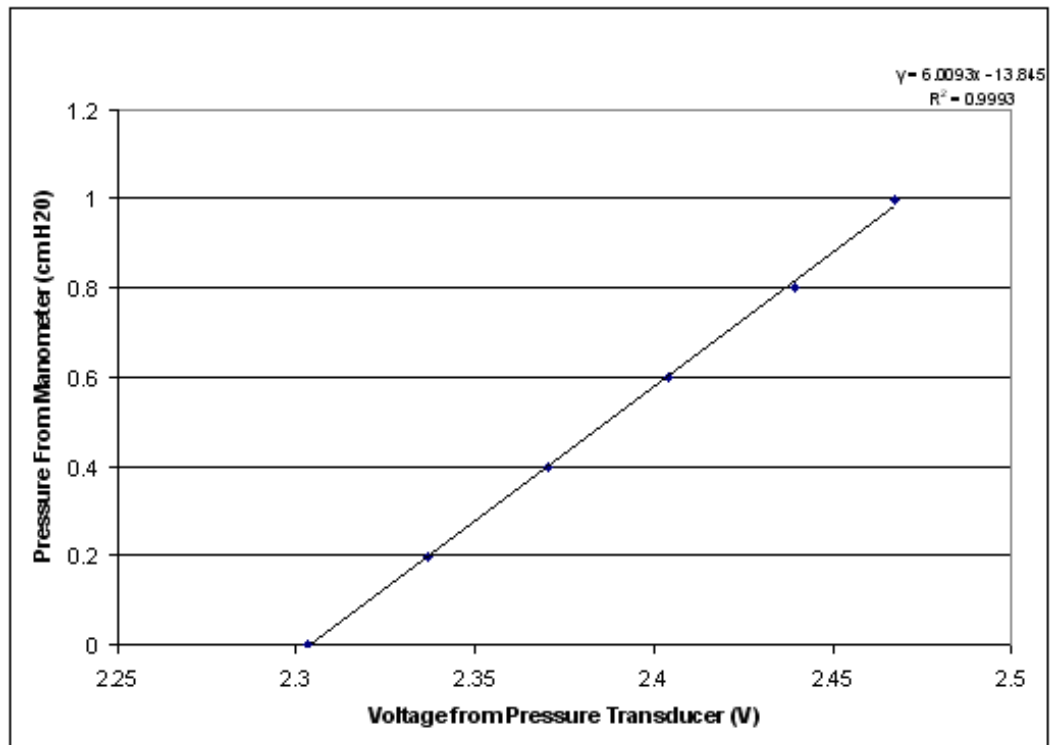
Figure 10. Comparison of Average Voltage Output from Pressure Transducer to
Pressure Values

The pressure – voltage relationship of the pressure transducer was determined from the equation derived in Figure 10. With a very high coefficient of determination ($R^2 = 0.9993$), the voltage to pressure transformation of the pressure transducer was determined to be linear in keeping with the design of many pressure transducers. In the program, the output of the voltage reading from the pressure transducer was converted to actual pressure readings using the linear regression model from this experiment (equation 3).

Equation 3: $Y = 6.0093X - 13.845$

Where: X = Output from forced MFM voltage values (V)
         Y = Pressure values (cmH2O)

4-1-3-1-3. Measured Pressure to Flow Comparison

A third procedure compared the pressure outputs to flow. Since the FP served as the flow standard, the pressure-flow calibration values provided by the manufacturer for the particular FP used (model number 3, Phipps and Bird; Richmond, VA) determined the flow outputs for pressure inputs. The manufacturer's FP calibration values are shown in Table 7.

Table 7. Fleisch Pneumotachograph Calibration Values

Pressure (mm H2O)	Flow (L/s)
1	0.858
5	4.29
10	8.254

The comparative equation for the pressure-flow relationship was determined from the calibration values given for the particular FP (Type 3) used. Figure 11 demonstrates the linear trend that is a trademark of FPs. The following equation was derived (equation 4).

Equation 4: $Y = 499.28X$

          Where: X = Pressure (cmH2O)
                     Y = Flow (L/min)
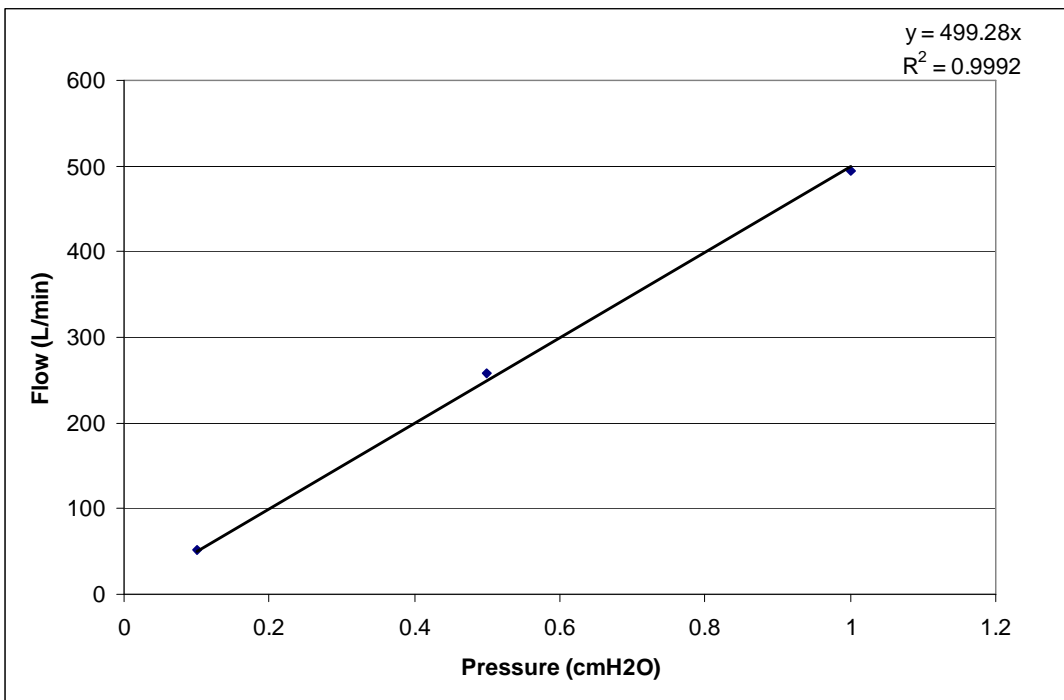
Figure 11. Pressure-Flow Comparative Curve for the Model Number 3 FP Used

As observed in Figure 11, the flow slope (499.28 L/min·cmH2O) indicates small changes in pressure for large flow values. This ratio dictates the sensitivity of the FP and consequently the sensitivity necessary for the pressure transducer.

4-1-3-2. Overall Accuracy and Calibration

To decrease the error accumulated over the subordinate steps that converted

pressure transducer voltage to flow (sections 4-1-3-1-1 to 4-1-3-1-3), the overall accuracy of the system was tested. The dynamic process used in this step is one that can be used in the future for calibrations of the MFM system. A breathing simulator device was chosen to simulate the breathing of a human subject. As shown in the setup (Figure 12), inhaled air passes through a tube where the MFM and FP are connected in series. The LabVIEW program was allowed to accumulate data for 30 seconds and the flow outputs of the two different types of flow meters were compared. A formula was derived for the MFM measured flow-flow relationship and incorporated within the program to compensate for any errors accumulated.
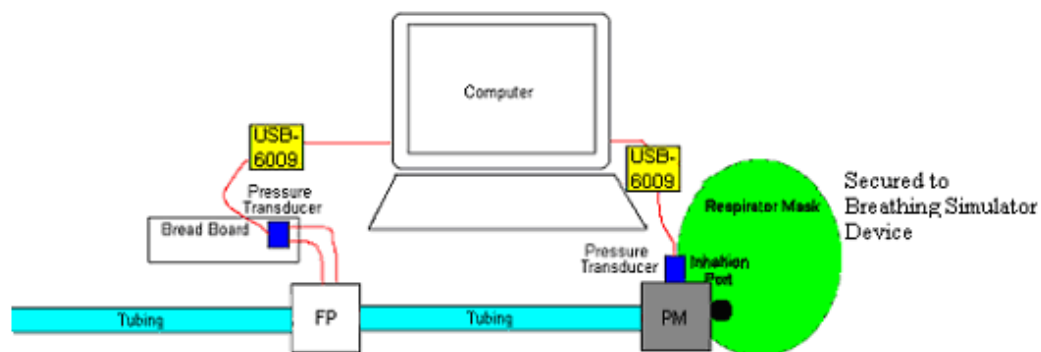
Figure 12. Breathing Simulator Device Setup with the Two Flow Meters

It was not possible to have several replicates of each test or to establish the relationship between the outputs of the two flow meters. The VPBS was not accurately adjusted and outputted values varied such that the maximal amplitude of the breathing waveform decreased with time. As such, the VPBS was allowed to operate for a duration equivalent to three trials (180 seconds) and all data points were utilized in the formulation process. The following results were obtained.

Upon inspection, the relationship between the two flow meters was seen to be linear (Figure 13). This was plausible given the incorporation of a polynomial relationship in the first transformation step (i.e., forcing the MFM output to be that of the FP). Indeed with a coefficient of determination of 0.9944, a nearly linear relationship was demonstrated between the two outputs. Upon closer examination, however, the non-linearity at both low (below MFM 20 L/min) and high flows (above MFM 118 L/min) was observed. This non-linearity could be due to the FP and/or the MFM. For this reason, a polynomial relationship was examined (Figure 14).
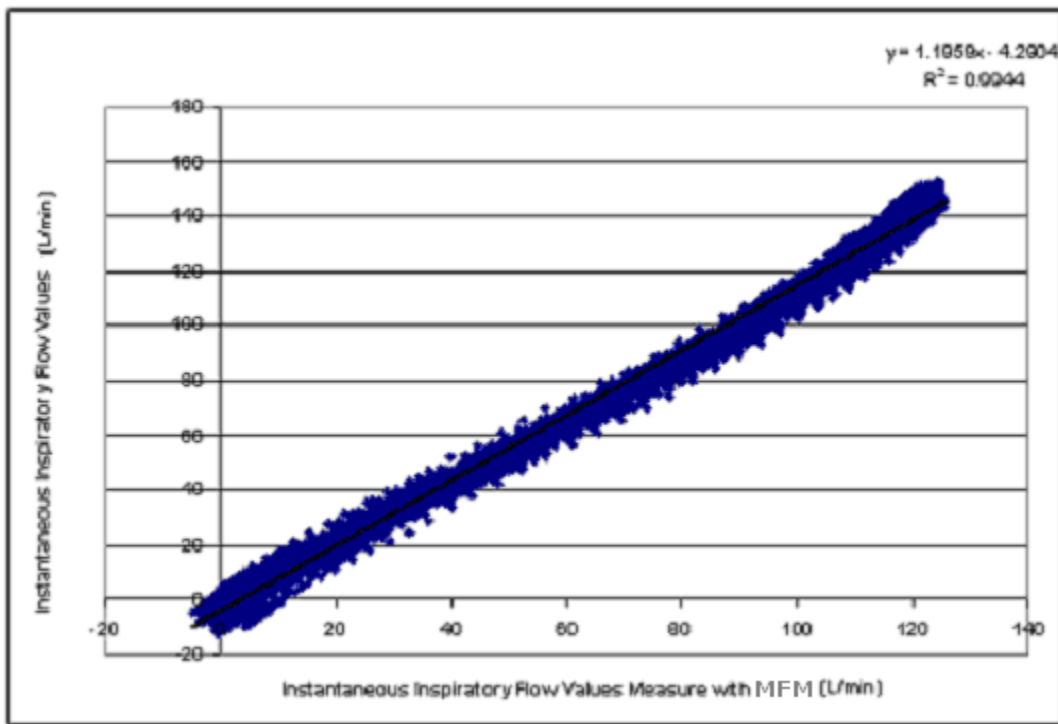
Figure 13. Dynamic Subordinate Calibration Results MFM for VPBS – Linear Relationship Highlighted
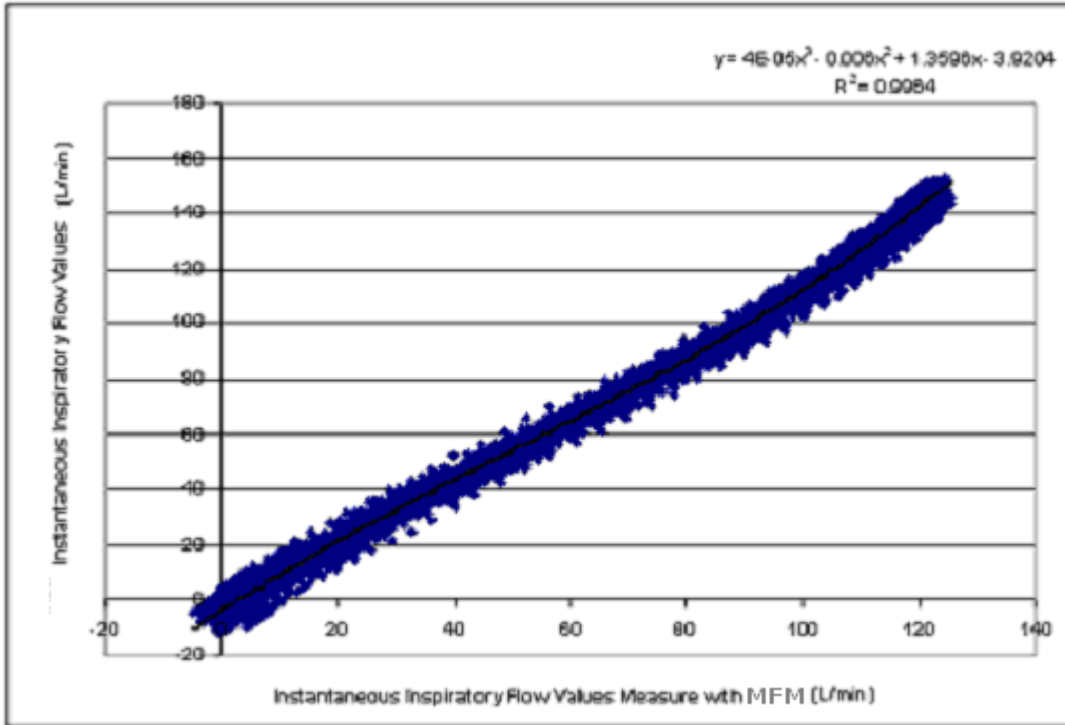
Figure 14. Dynamic Subordinate Calibration Results MFM for VPBS – Polynomial Relationship Highlighted

A slight increase in the correlation of determination value (+0.002) is seen in the polynomial relationship, suggesting that although a linear formula would suffice, a slight increase in accuracy was gained using a polynomial fit. The coefficients of each term in the polynomial can indicate the role of that particular factor at a given point. For example, the 0.00004 coefficient for X^3 shows that the relationship between the two meters can be described as cubic, but that the coefficient for X and constant values dominate the output. Interestingly, while the offset was reduced, the span was increased as the relationship was transformed from a linear to a polynomial curve. These factors corroborate the assumption that the relationship between the two meters is generally linear.

The polynomial relationship below was used in the program as the final

54

formula to account for any non-linearity.

Equation 5: $\qquad Y = 0.00004X^3 - 0.006X^2 + 1.3596X - 3.9204$

$\qquad$ Where: X = MFM Inspiratory flow (L/min)
$\qquad\qquad$ Y = Inspiratory flow (L/min)

As mentioned previously, this process was used as a quality control method for premeditating any systemic errors in the system. Given that three equations were used to convert the voltage output of MFM pressure transducer to a flow approximating the FP, there is a risk that errors have accumulated and propagated through the system. Incorporation of Equation 5, therefore, is one method that was used to reduce errors.

The American Thoracic Society (1995) recommends calibration of the flow meter system at least daily. If a dynamic calibration procedure, like the dynamic procedure described above is not possible, then calibration with a 3-L syringe is advised. With a syringe, the injections and withdrawals are completed separately. Withdrawals from the syringe are equivalent to inhaled air, while injections are the equivalent exhalations. With the syringe connected to the system, and no flow applied, the average of the data accumulated is the zero off-set. To determine the span, the syringe injects air into the system and the flow values are integrated to obtain the volume. This volume is then compared with the volume of the syringe thus forming the span. Every six months, different flows should be tested with the volume syringe. That is, the flow rate should be changed between 2 and 12L/s. That is, a volume of 3 liters must be injected in approximately 1, 6, and between 2 and 6 seconds. Note that some practice is required to produce a constant flow.

It is also recommended that this calibration procedure be performed in the environment where the system is to be utilized. This is particularly important in environments where the ambient temperature is constantly changing where the syringe is acclimatized to both temperature and humidity (American Thoracic Society, 1995).

4-2. Experimental Design

The system was validated with a series of test by VPBS and human subject tested at rest and at 85% of their age-predicted maximum heart rate.

4-2-1. Simulated Breathing Tests

The VPBS was used to mimic the natural breathing of a human as selected by various breathing profiles. By selecting a profile (Table 9), the respiratory response due to various work loads and stresses was simulated. The advantage of using this machine is its ability for selecting various breathing profiles without the requirement of inducing stressful work loads on a human subject. Another advantage is the ability to repeat tests with a high degree of accuracy.

The operation of a VPBS relies on incremental changes to the volume of a welded stainless steel bellows. The changes are made by a processor controlled operation of a lead screw drive system. The user can alter the profile, breaths per minute (BPM) and amplitude to attain the respiratory conditions desired. The profile is the pattern of changes to the screw drive system programmed into the processor. The BPM or breaths per minute is altered with an internal potentiometer. Lastly, the amplitude is the percentage increase in a profile's simulated flow rate at a particular BPM and was altered from 50% to 100%. This allows scaling of the inspiratory

volume flow rate to suit a particular need. The specifications of the VPBS are shown in Tables 8 and 9.

Table 8. VPBS Specifications (Krug's Life Science, KRUG International Company; San Antonio, TX)

Maximum Flow Rate	450 liter/min (STP)
Breath Rate	2 to 50 BPM
Maximum Stroke Volume	6.757 liters
Volume Resolution	1.622 ml

Where: Maximum Flow Rate: Maximum flow rate possible
            Breath Rate: Maximum rate of inhalation and exhalation
            Maximum Stroke Volume: Maximum volume displaced by bellows
            Volume Resolution: Volumetric tolerance of the steel bellows

Table 9. VPBS Profiles Breathing Characteristics (Krug's Life Science, KRUG International Company; San Antonio, TX)

Profile	Breath Cycle Shape	Volume Flow Rate (L/min)	Breaths Per Minute	Volume per Breath (L)
1	Sinusoidal	33.3	30	10.5
2	Sinusoidal	100	30	31.8
3	Sinusoidal	300	30	96

Three different profiles, or pre-set breathing characteristics, were available on the VPBS. In all experimental setups, VPBS profile number 3 was used to provide the maximum flow rate possible within the normal sinusoidal breath cycle and therefore maximum challenge to the MFM system. The amplitude was adjusted between 50% and 100% to adjust the maximal flow rate. At 50% amplitude for profile 3, the maximum flow should be approximately 150 L/min. At 100% of the

amplitude, the maximum flow should was to be 300 L/min. Attempts were made to operate the VPBS at 150% of the amplitude of profile 3, at 450 L/min. The condition of the machine, however, did not permit such high flow rates.

4-2-2. Human Subject Tests

4-2-2-1. Subject Recruitment

Ten untrained subjects were chosen based on a voluntary agreement of participation and overall health conditions. As the American College of Sports Medicine (6th edition, 2000) states, medical clearance for those within the age group of 18 to 40 years is not required. Only participants that fell within this age group were chosen (Table 10).

Table 10. Demographic Information for Subject Participants

Subject #	Gender	Height (cm)	Weight (Kg)	Age	Calculated Maximum Heart Rate (beats/min)	Measured Resting Heart Rate (beats/min)	Calculated Target Heart Rate (beats/min)
1	Female	165	65.3	26	194	84	177.5
2	Male	174	68.1	24	196	75	177.85
3	Female	172	65.7	33	187	79	170.8
4	Male	174	79.8	34	186	68	168.3
5	Male	172	83.9	29	191	82	174.65
6	Female	168	56.2	22	198	74	179.4
7	Female	169	73.9	24	196	70	177.1
8	Female	168	49.9	25	195	66	175.65
9	Female	163	66.7	25	195	78	177.45
10	Female	176.5	74.4	25	195	74	176.85

Note: Calculations for maximum heart rate and target heart rate are shown in equations 6 and 7.

Prior to performing any subject testing, the subjects were invited to participate

in the orientation session. At this time, the subjects were given an overview of the

objective and methods of test sessions. They also received a written consent form

and a brief medical history document. The written consent form (Appendix B)

highlighted the procedures and methods of the tests. The brief medical questionnaire

(Appendix C) was used to gather information on previous and currently known

medical conditions that might make testing unsafe for the subject. Completed forms

were reviewed by the testing coordinator and the subjects were selected based on

overall health criteria.   In particular, subjects were screened for cardiovascular

problems and respiratory conditions. As no medical conditions that could imply

health risks were identified in the orientation sessions, all subjects who initially

volunteered were allowed to proceed to testing.

4-2-2-2.Test Set-up

Each subject was recruited for the completion of two separate procedures on

multiple days: measurement of breathing while at rest and during exercise. As such,

there were two separate test setups, each described in the sections below.

4-2-2-2-1 Test Set-up – Breathing While at Rest

The purpose of this test was to show the MFM's accuracy in measurement of

inspiratory flow rates of subjects. As before, the FP flow was deemed the true flow

and a human subject wearing a respirator mask was the flow source instead of the

VPBS (Figure 12).   The respirator mask was worn by a human subject sitting on a

chair to allow for a respiratory rate of a sedentary individual. A picture of the setup is

in Figure 15.

Figure 15. Human Subject Testing of Breathing While at Rest

4-2-2-2-2 Test Set-up – Breathing During Exercise at 85% Age Predicted
Maximum Heart Rate

The purpose of this test was to show the feasibility of taking measurements of

subject running on a treadmill to determine the ability of the MFM to capture

complex breathing patterns. To demonstrate the usage of the MFM in a real setting, it

was connected to a C2A1 carbon filter canister and M40A1 respirator mask only. No

FP was used to compare flow rates in this setup (Figure 16).

Figure 16. Human Subject Testing of Breathing during Exercise at 85% Age Predicted Maximum Heart Rate

4-2-2-3. Testing Procedures

Participants were invited to the laboratory for testing on two separate occasions for a sedentary and exercising test sessions. To complete a sedentary breathing test, the test was similar to that in Figures 6 and 7. Each volunteer was asked to be seated on a chair for five minutes. This allowed the subjects to establish a resting heart rate and dissipate any possible anxiety regarding donning a respirator mask. After five minutes, the subjects were given their respirator mask. The test coordinator helped the subjects in donning the M40A1 and insured a snug but comfortable fit. The LabVIEW program was initiated and data were collected for

sixty seconds at fifty Hertz. The data were saved to a particular file for analysis with only the subject number and the testing condition (ie. "subject1sitting"), thus ensuring privacy.

To measure inspiratory flow characteristics during exercise, volunteers were asked to return to the laboratory for a second testing session. The participants were fitted with a heart rate monitor (Polar Electro Oy; Kemple, Finland). The monitor consisted of an electrode band worn around the chest and a wireless wrist monitor indicating the heart rate. Resting heart rates and 85% of their age predicted maximal heart rates (target heart rate) were determined. The equations below (equations 6 and 7) were used to calculate the age predicted maximum and target heart rates.

Equation 6: $HR_{max} = 220 - age$ (Johnson, 1999)

Where: HR max = age predicted maximum heart rate (beats/min)

Age = age of human subject (years)

Equation 7:   Target Heart Rate $= [(HR_{max} - HR_{rest})*0.85] + HR_{rest}$

Where: HR_{rest} = Resting heart rate (beats/min)

These heart rate values were obtained to elicit the desired work rate of moderate and high levels expected in a real world setting. This particular rate of exercise was chosen to elicit the highest occurrence of PIFs without overstressing the subjects.

To reduce cardiovascular stress, participants' heart rates were monitored through a five minute warm up period. The subjects were asked to straddle the belt of a Quinton (Bothell, WA) motorized treadmill. The belt was started and the subjects were asked to step carefully onto the moving belt. The speed and grade of the

treadmill was then increased gradually to enable the subject to reach approximately 50% to 60% of their age predicted maximal heart rate. After five minutes, the belt was stopped.

Immediately pursuant to this warm up period, subjects were seated and fitted with a respirator mask, MFM and carbon filter canister. Hoses were not necessary in this session as inspiratory flow measurements were made only with the MFM. The MFM was connected to the USB6009 and pressure transducer, and the program was initiated. The subject was then allowed to start jogging on the treadmill. The speed and grade of the treadmill were increased once per two minutes such that the person reached their target heart rate. Once the target heart rate was attained, the speed and grade were held constant and data were obtained for approximately 60 seconds. When the target heart rate was reached, the program was allowed to log data for roughly 60 seconds. Other reasons for cessation of experiments could be indications by the subject such as abnormal and sudden increase in heart rate, difficulty in breathing and/or paleness. Finally, the experiments could be truncated due to the volunteer's request to terminate the test. Across the board, the duration of experiments conducted with subjects were 60 seconds and not terminated due to voluntary cessation.

4-3. Data Collection and Analysis

The computer program (Appendix D) was initiated once subjects reached their unique target heart rates and terminated due to time limits (reaching 60 seconds) or voluntary termination. In this way, the warm up and recovery periods were not used in the data. As the main purpose of this project is to determine the PIF, data from the

entire 60 second duration of exercise were examined. In each output Excel file, the time, pressure and flow values for each subject were recorded at the specified sampling rate along with a time stamp.

As the data were sampled at a rate of 50 Hz, large amounts of data were obtained for each trial. In some cases, exercise duration was greater than 60 seconds. In those cases, data taken after the sixty second mark was removed from analysis. The methods, described below, were used to analyze the pertinent data.

4-3-1. Breath by Breath Analysis

The method of data analysis was chosen to be similar to a novel approach used by Coyne et al. (2006). In this approach, the data were examined breath by breath, where a breath is defined as a complete inhalation and exhalation. As the MFM was connected to the valved inhalation port of the respirator mask, only inhalation values were used. The exhalation values were shown as approximating zero flow and were removed from analysis. The instantaneous inspiratory flow rate data points were analyzed to determine the PIF and average inspired minute ventilation value (VI_{avg}).

The beginning and end of each breath were determined by a series of IF-THEN statements in Excel. The results of these IF-THEN statements were gauged for accuracy with visual representations of the instantaneous flow. The PIF was determined as the highest instantaneous inspiratory flow rate data point from each inhalation period. The VI_{avg} was calculated as the average of all instantaneous inspiratory flow rate data points in a given inhalation period.

The PIF was obtained by obtaining the maximum instantaneous inspiratory

flow rate for each breath. The maximum PIF was the calculated as the maximum PIF for each subject experimentation session and the PIF_{avg} measured by averaging the PIF values.

4-3-2. Statistical Analysis

Statistical analysis was performed on the data to determine the difference between the MFM and the industry standard FP. In this case, there are two treatments, MFM and FP, as well as two dependent variables, PIF and VI_{avg}. To assess the accuracy of the program results from the labVIEW program for the MFM, it must be gauged against the FP results. Two statistical tests were used for this purpose: goodness of fit test and t-test.

4-3-2-1. Goodness of fit test

The goodness of fit test is measured by a coefficient of determination, R^2. This value is an indication of the agreement of the measured values to the true values. In this case, the measured values were from the MFM and the true values from FP. The coefficient of determination was used to determine the amount of variance between the measured value and true value. This value is best for linear relationships.

4-3-2-1. t-Test

A simple t-test can compare the statistical significance of sample means. A t-test was chosen as the method of statistical analysis. This test is particularly well suited as it can be used even when the sample size is low. Indeed, it can be used for sample sizes of 10 or less. Furthermore, the assumptions of this test are well suited to the characteristics of this project. One of the assumptions of the t-test is that the errors are normally distributed within each group. Finally, the samples can be

independent or dependent. Independent samples are two randomly selected sample groups. Dependent samples, on the other hand, are either two sample groups that are matched on the same variable or one sample group that is tested twice (ie. before and after treatment tests). For this reason, an independent t-test is chosen. As the difference can be either positive or negative, a two-tailed t-test is preferred (Ott and Longnecker, 2001).

Data analysis was performed using Microsoft Excel. The probability of Type I error was used to determine if variations between the two flow meters are due to real differences or due to random noise. In other words, this is the probability that there is no difference between the two groups or flow meters. The results were interpreted by evaluations of the level of significance value referred to as p value. T-tests are often evaluated at a 5% significance level. That is, the p value obtained from the t-test is compared against a tabled value at p=0.05 to determine its statistical significance. For p values of 0.05 or less, statistical significance is present between the two samples being compared. In this study, p values of 0.05 or greater are desired to demonstrate statistical insignificant differences between the two treatments, the true flow as measured by the FP and the measured flow from the MFM.

Chapter 5: Results and Discussion

5-1. Final Data Acquisition System

In the final design, the mask flow meter system comprised MFM body, 5-inch-d-4v pressure sensor, Dell Latitude D505 laptop, USB6009 data acquisition card and connection wires. The final version of the program used in this study, converted the raw voltage output from the MFM pressure transducer to flow with one equation, equation 9. This equation was derived by merging the data from several subordinate steps. Specifically, measured voltage and flow data from steady state, breathing machine at low and high flow levels, as well as human subjects at rest were combined. The overall MFM measured voltage and flow relationship was obtained (Figure 17).

$$y = 6311.6x^3 - 48583x^2 + 125422x - 108240$$
$$R^2 = 0.9963$$
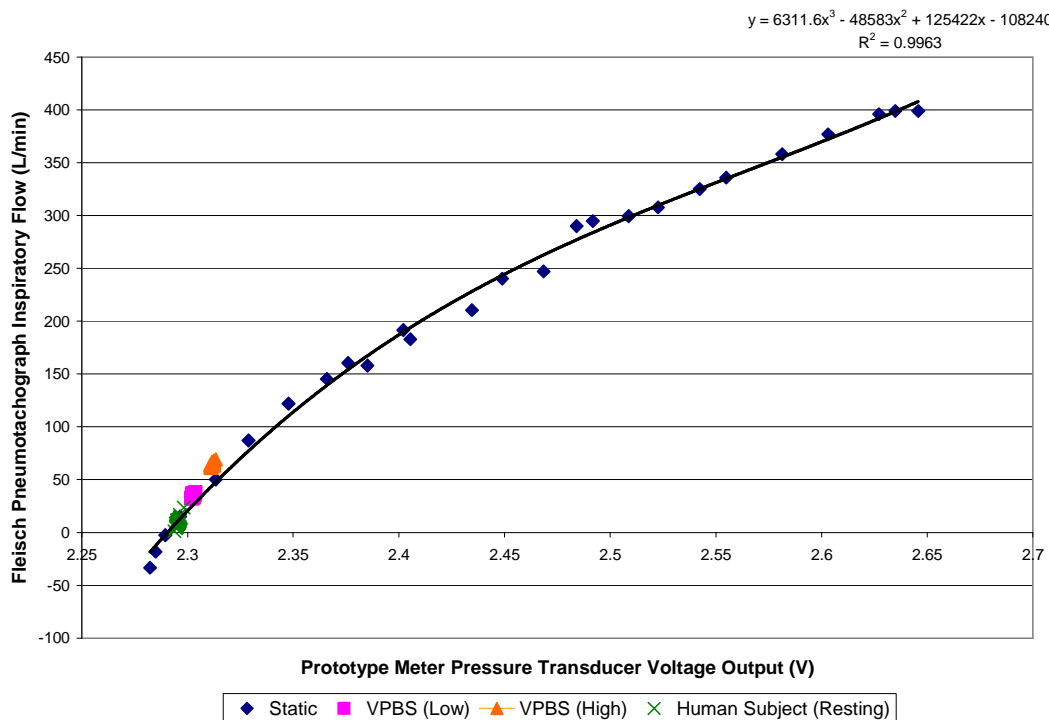
Figure 17. Accuracy Assessment of Data Pooled from Steady State, Variable Profile Breathing Simulator device (VPBS) and Human Subject Testing While at Rest

From Figure 17, it can be seen that there are three non-convergent clusters that fall on a large range of flow obtained from static flow conditions. Significantly, the clusters appear at different sections of the steady state MFM voltage and flow curve. This was explained by the difference in the average flow value of each cluster; the average inspiratory flow of human subject resting is 9.14 L/min, low flow VPBS is at 34.95 L/min and high flow VPBS is at 64.45 L/min.

The measured voltage-flow relationship is encompassed by the third order polynomial below (Equation 9). This equation was used in the final version of the virtual instrument program.

Equation 9: $Y = 6311.6X^3 - 48583X^2 + 125422X - 108240$

Where: X = Voltage from the MFM pressure transducer (V)
Y = Flow (L/min)

With a coefficient of determination of 0.9963, the equation was deemed to accurately depict the MFM voltage-flow relationship. The large constant coefficients indicate small changes in the voltage correlate to large changes in the flow. Therefore, a very accurate system is needed since pressure transducer errors at a very small order of magnitude can affect the measured flow output.   The pressure transducer manufacturer has specified a $\pm$ 0.06 V accuracy due to temperature fluctuations, $\pm$ 0.01 V accuracy for measurements made prior to pressure transducer warm up, and $\pm$ 0.005 V due to positioning. According to the specifications, the largest possible alteration from true flow is due to the temperature fluctuation and should be avoided. Calibration should be completed in the location where the MFM will be used to avoid fluctuations in the flow due to temperature.

5-2. Simulated Breathing Tests

Following the incorporation of the formula obtained from the dynamic calibration into the program, the system was prepared for testing. The most reliable method of testing is that of simulated breathing by a machine for which a highly predictable breathing pattern was established. The predictable breathing pattern provides a control and is the key to highlighting errors, if any, in flow measurements made by the MFM. The predictable breathing pattern establishes a known reference point against which anomalies may be more easily detected (Figure 18).
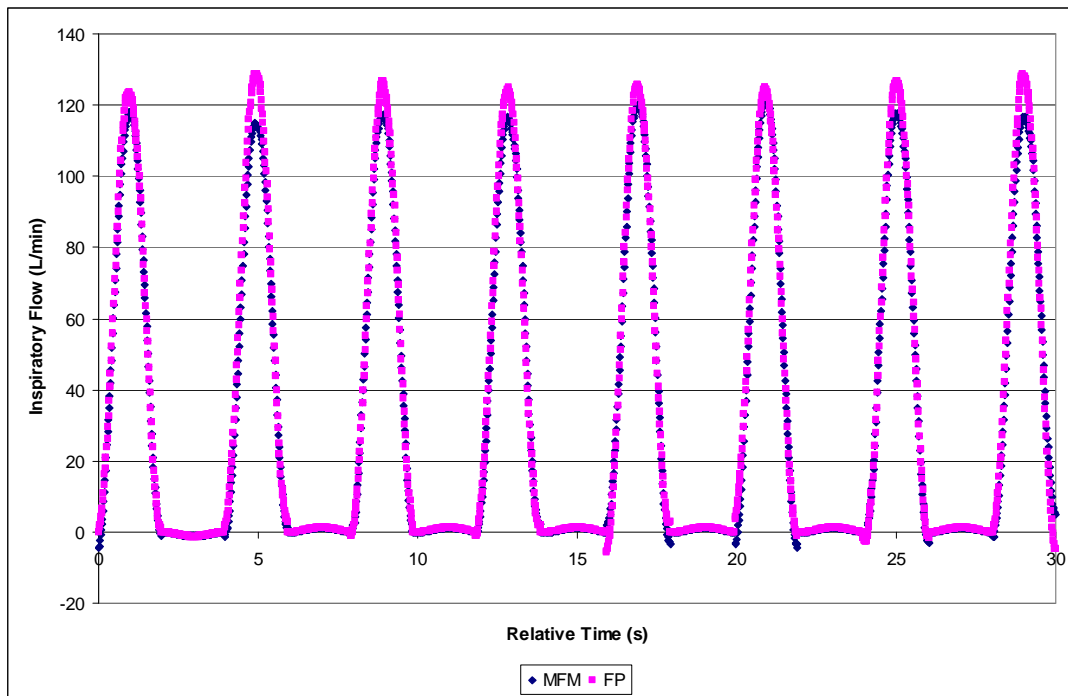
Figure 18. Sample VPBS Inspiratory Flow as Measured by Both MFM and FP

Tests were completed at the lowest and highest possible flow rates by the Krug VPBS. The VI_{avg} (Figure 19) and PIF (Figure 20) were calculated for each flow condition. A sample of the instantaneous flow versus time output is in Appendix H.
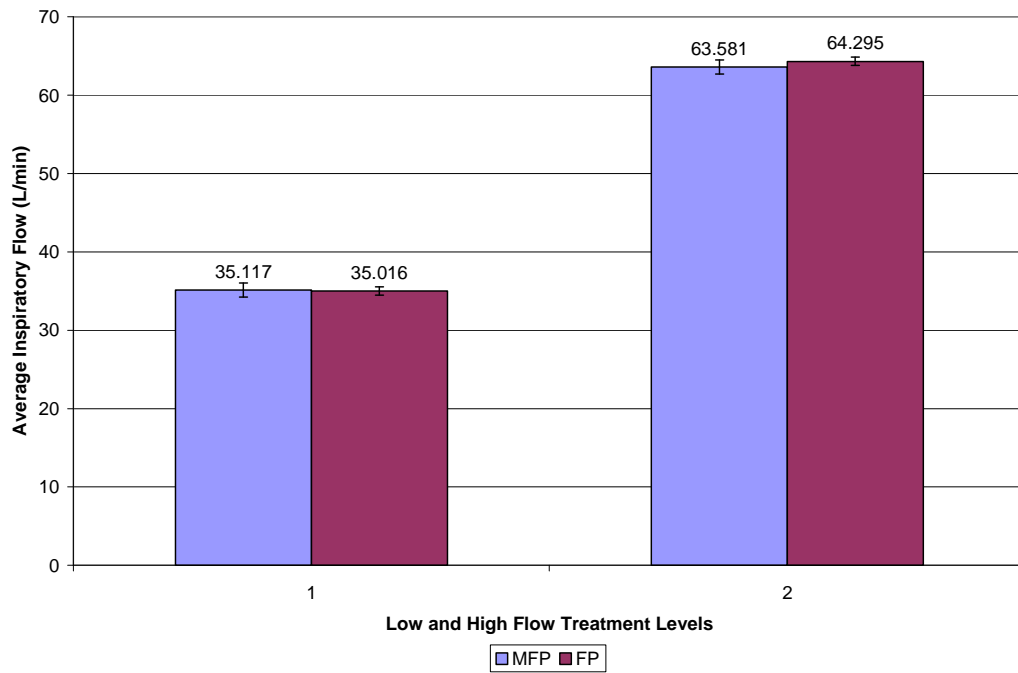
Figure 19. Average Inspiratory Flow of VPBS at High and Low Flow rates as Measured by the MFM and FP
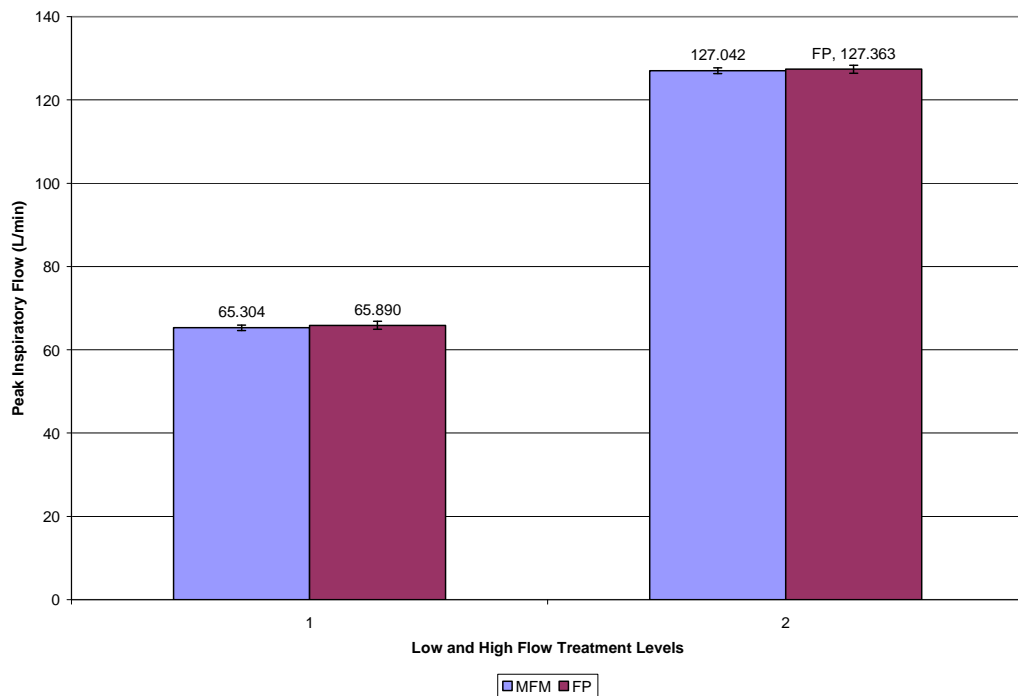
Figure 20. Average Peak Inspiratory Flow of VPBS at High and Low Flow rates as Measured by the MFM and FP

The figures above illustrate that measurements made by the MFM and FP are

very similar and have very low standard deviations. The variability of measurements were higher in the MFM (SD = 0.891) than the FP (SD = 0.538) for VI_{avg}. In measurements of average PIF, however, the FP (SD = 0.952) had a higher variability than the MFM (SD = 0.689).

The accuracy of measurements made by the MFM was gauged with a t-test. The results indicating the p values and the level of statistical significance are shown in Table 11. Without exception, the p values indicate that there is no significant difference between the MFM and flow values in measuring both the VI_{avg} and average PIF.

Table 11. Statistical Significance of Average Inspiratory Flow and Average Peak Inspiratory Flow of VPBS at Low and High Flow Rates

Condition	T-test P-value Results for Average Inspiratory Flow Rate	T-test P-value Results for Average PIF
VPBS Low Flow Trial 1	0.602909	0.055952
VPBS Low Flow Trial 2	0.202728	0.499695
VPBS Low Flow Trial 3	0.268263	0.057367
VPBS High Flow Trial 1	0.207421	0.364375
VPBS High Flow Trial 2	0.057929	0.138936
VPBS High Flow Trial 3	0.189835	0.183323

5-3. Subject Tests

Subject testing was the final measure of the usability of this flow meter. The

71

goal of the first set of experiments was to test the accuracy of the flow meter in

measuring VI_{avg} and PIF of seated subjects at resting heart rates (Figure 21).
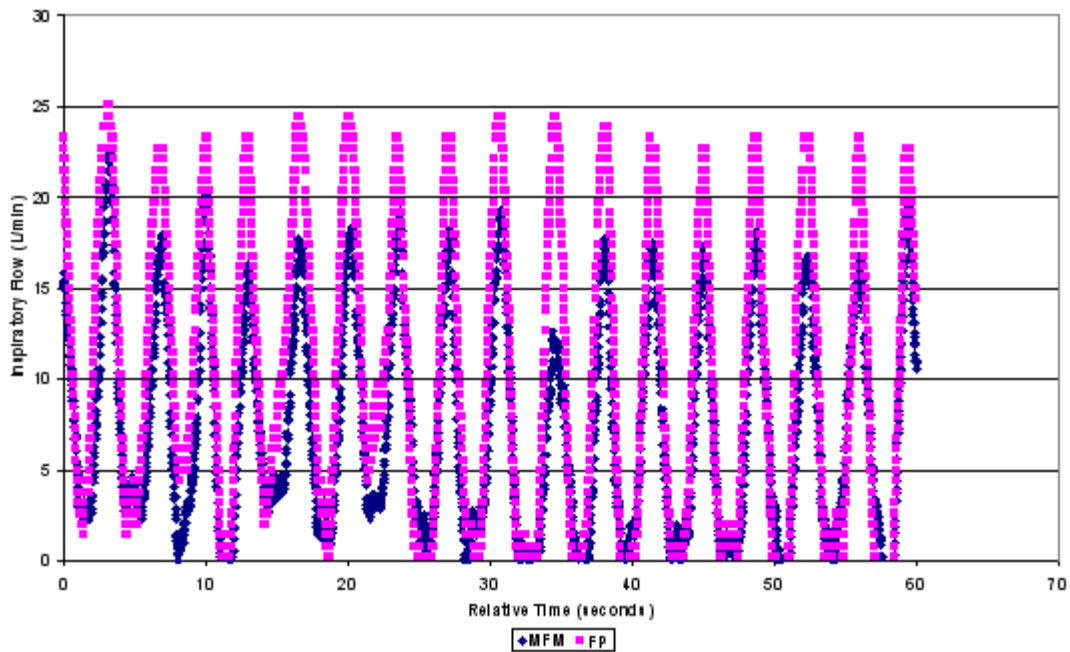
Figure 21: Example of Instantaneous Inspiratory Measured for a Single Study Participant at Resting Heart Rate

The second set of experiments was used to determine the VI_{avg} and PIF in

subjects at 85% of their age-predicted maximum heart rate (Figure 22).

The physical demand placed on the individuals was reflected in their

respiratory response. The VI_{avg} rate was increased in all cases at a higher work load.

PIF, likewise, increased with an increase in workloads.
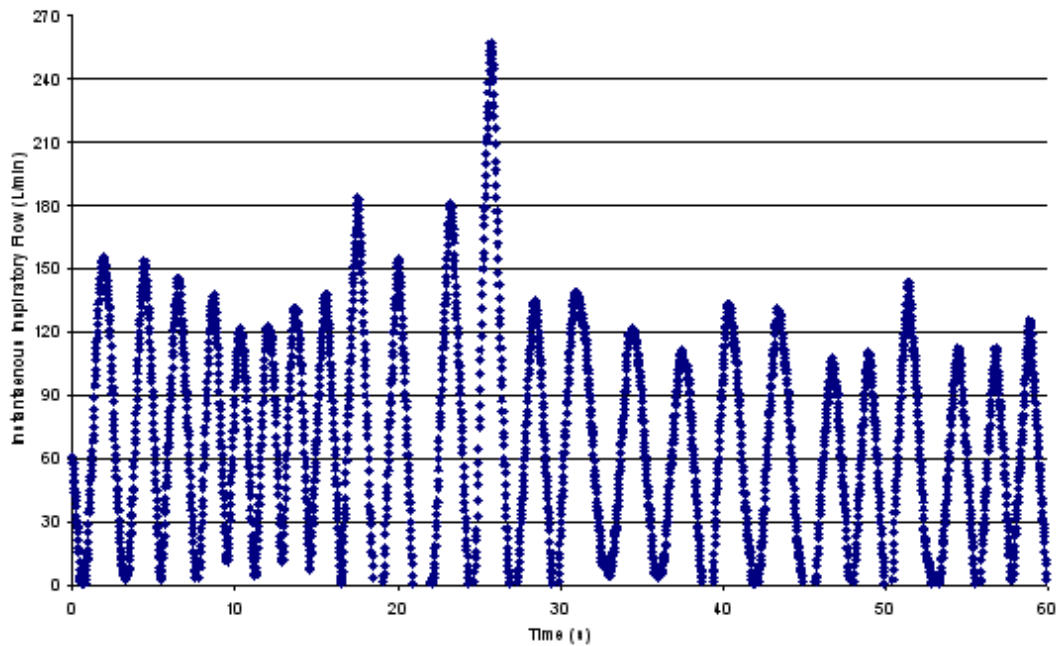
F
igure 22: Example of Instantaneous Inspiratory Measured Flow for a Single Study Participant at 85% of Age Predicted Maximum Heart Rate as Measured by MFM

Table 12 summarizes the results determined from these two tests. The complete set of breath by breath data and a sample of the instantaneous flow versus time output is available in Appendix I.

Across the board, the VI_{avg} values obtained from both flow meters were lower than expected. The average resting inspiratory flow rate of all subjects was 8.72 L/min. Although the values were lower than expected, the average resting flow rate was higher for females (9.30 L/min) than males (6.96 L/min). At 85% of the age predicted maximum heart rate, all subjects were running, and the average flow was 51.03 L/min for all subjects. Again, the females (52.28 L/min) had a slightly higher flow rate than the males (47.28 L/min).

Table 12. Average and Peak Inspiratory Flow of Subjects at Resting and 85% of their age-predicted maximum heart rate as measured with the MFM and FP

		At Rest				At 85% Age Predicted Maximum Heart Rate	
		Average Inspiratory Flow (L/min)		Average Peak Inspiratory Flow (L/min)		Average Inspiratory Flow (L/min)	Average Peak Inspiratory Flow (L/min)
Measurement		MFM	Flow	MFM	Flow	MFM	Flow
Subject	**Gender**						
1	Female	9.63	10.33	21.72	23.63	66.98	140.72
2	Male	5.28	5.04	8.47	9.25	56.77	124.7
3	Female	11.07	36.63	15.05	37.42	56.69	110.77
4	Male	8.65	11.76	28.62	29.24	37.8	73.85
5	Male	14.6	15.1	24.8	25.6	81.47	139.9
6	Female	10.76	10.35	17.56	18.17	67.8	135.14
7	Female	8.47	8.91	15.14	16.72	17.25	36.9
8	Female	8.56	9.28	18.3	19.4	55.15	117.84
9	Female	8.12	8.37	13.65	14.1	42.88	73.66
10	Female	10.27	10.44	17.65	18.14	63.65	104.05

It follows that the average PIF values were also lower than expected. At rest, the average PIF values were 18.58 L/min. Interestingly, the values for female subjects (average PIF = 18.36) was lower than for male subjects (average PIF = 19.24). At 85% of the age predicted maximum heart rate, all subjects were running, and the average flow was 100.86 L/min for all subjects (female subjects' average PIF = 101.39 L/min; male subjects' average PIF = 99.28 L/min).

The discrepancies described above in the average flow rate and PIF may be the result of inherent variability of breath by breath data analysis that can arise from

biological variability and high sampling frequency (Myers et al., 1990). However, it

may possibly be attributed to systematic errors. This discrepancy was examined by

analyzing the two parameters using a t-test for resting conditions only (Table 13).

Table 13. Statistical Significance for Average Inspiratory Flow and Average Peak
Inspiratory Flow Rate of Subjects at Rest

	p value from t-test	
Subjects	Average Inspiratory Flow	Average PIF
1	0.3676	1.08E-08
2	0.586	0.50429
3	0.3788	0.8432
4	0.1568	0.9168
5	0.4158	0.185
6	0.4919	0.596
7	0.09803	0.000241
8	0.340066	0.403466
9	0.305877	0.120451
10	0.746049	0.5365

With the exception of two cases, subjects 1 and 7, all results indicated that

there were no statistically significant differences found in the measurement of VI_{avg}

and average PIF. The average p value for VI_{avg} (p = 0.386) and average PIF (p =

0.385) indicate there was essentially no difference in the ability of the MFM to

measure VI_{avg} and average PIF. This result was consistent with the VPBS tests; at

low flow rates, the MFM meter may be considered as accurate as the FP.

At higher flow rates, it was not possible to perform a t-test as the FP was not

connected to the respirator mask. Therefore, the ratio of maximum PIF to VI_{avg} rate

was used as an alternative metric to assess the accuracy of the MFM at higher work

rates (Table 14).

Table 14. Maximum PIF and Maximum PIF to Average Inspiratory Flow Rate
Average for subjects at 85% Age Predicted Maximum Heart Rate Work Load

Subjects	85% Age Predicted Maximum Heart Rate	
	Maximum PIF (L/min)	(Maximum PIF/ Average Inspiratory Flow Rate) Ratio
1	254.03	3.793
2	136.07	2.397
3	230.9	4.07
4	153.91	4.072
5	172.79	2.12
6	166.36	2.454
7	40.51	2.348
8	218.03	3.953
9	90.95	2.121
10	122.24	1.921
Average:	147.76	2.882

The average maximum PIF value was 147.76 L/min, with the highest value

from subject 1. Observations from the flow rate values of subject 1 revealed a sharp

increase in inspiratory flow. Post experimental comments from the subject revealed

that the subject felt uncomfortable at this time and needed a higher inhalation to

overcome fear of receiving insufficient oxygen. Subject 7, on the other hand, had an

astonishingly low PIF compared to all others. Post experimental comments from the

subjects revealed that the subject is a SCUBA diver and has trained herself to have

low flow rates and therefore consume less oxygen.

The average ratio of maximum PIF and VI_{avg} was 2.882. This value correlates with literature findings in which the average ratio of PIF to VI_{avg} typically ranges from 2.5 to 3.8 with values decreasing at higher work rates (Jansen, Anderson and Cassidy et al., 2005 and Johnson, 2005). From the low ratio, it was reasonably concluded that the subjects were under respiratory stress on average despite the low VI_{avg} at the higher work rate. Furthermore, it is possible to presume the MFM to be accurate in measuring the maximum PIF and VI_{avg} at higher work loads.

Chapter 6: Conclusions and Future Considerations

The main goal of this study was to provide a means to measure the PIF and VI_{avg} of a subject wearing an M40A1 respirator mask and C2A1 carbon filter canister. The objectives numerated below were successfully fulfilled with a portable flow meter system comprised MFM body, an All Sensors' 5-inch-d-4v pressure sensor, Dell Latitude D505 laptop, National Instrument's USB6009 data acquisition card and 10 pin connection wires. The MFM successfully:

1) Provided a safe and portable miniature measurement device that accurately measured the VI_{avg} and the PIF without compromising the integrity of the system seals or placing undue stress upon the user.

2) Provided a data acquisition system that obtained and stored PIF and VI_{avg} in such a manner as to allow data manipulation for statistical analysis.

3) Ensured measurement accuracy of the flow meter system with laboratory experiments including steady state flow, VPBS at low and high flow rates, as well as human subject testing at rest and at 85% of age predicted maximum heart rate.

The MFM body was connected to the M40A1 respirator mask and C2A1 carbon filter canister with unique NIOSH threads. With a Microsoft Excel format, manipulation and statistical analysis of the system data output was possible. Indeed, across the board, a high degree of accuracy of $\pm$ 0.02% was revealed in a breath by breath comparison of the measured VI_{avg} and PIF data and true flow values.

6-1. Future Consideration

Overall this study was successful in attaining its objective. In the process of achieving the goals, two avenues were identified that could be taken to explore the

results of this project to the fullest extent possible. The first is further examination of processes and results discussed in this project. The second is further examination of applications of usage of this system. Each is discussed below.

6-1-1. Examination of Current Methods and Results

First, calibration setups can be re-examined for measurement variations due to the effect of carbon filter and pressure transducer placement, as well as accuracy of VPBS utilized.   Second, human subject experimental data can be supplemented with tests at 85% of VO2 max exercise levels to verify that 85% of age predicted maximum heart rate properly elicited respiratory stress in subjects. As the current method tested 7 female subjects, and 3 male subjects, a more even distribution of female and male subjects can be tested to avoid gender-skewed results. Additionally, the setup used for seated subject testing can be modified for use in exercise testing such that both meters are used at the higher work loads. The validity of the system can be investigated in a real world setting, outside of the laboratory. The system was designed to be portable, and it is best to test the system in the setting for which it was intended. Finally, given the technology level of PDAs and or small notebook computers, the program can be transferred to a smaller footprint or handheld system.

6-1-2. Examination of Applications

Aside from usage of this system for determination of the respiratory stress associated with certain tasks, this system can be used to disentangle several misconceptions regarding the influx of contaminants that concerns respirator users. These concerns fall into two categories. The first concern is the filtering capacity of carbon filter canister during usage. By correlating the occurrence of PIF and accurate

VI_{avg} of certain tasks, one can determine the exact volume of air passing through the carbon filter canister over a period of interest and thus determine the true lifecycle of the canister. The second concern is the sealing capabilities of respirator masks. This system can be to determine the presence of leakage in respirator masks. With slight modifications, this system can be used in both the inhalation and exhalation ports of M40 respirator mask. With preliminary studies to determine the difference between the inspiratory and expiratory average flow volumes, instantaneous leakage can be identified.

6-2. Conclusions

A flow meter system was devised such that it satisfied the study goals. The system comprised a portable, pressure-differential wire mesh resistance flow meter attached by NIOSH threads between the M40A1 respirator mask and C2A1 cartridge. Voltage output from a pressure transducer connected to the flow meter was used to derive the instantaneous flow through a series of data transformative steps in a virtual instruments program.

Appendix

Appendix A – Engineering Drawings

6 Pressure Sensor

5 Rubber Seals

4 Gasket

7 PVC Spacer

3 Mesh Filter

2 Inner Tubes

1 Body

Assembly

Flowmeter Design

Shaya Jamshidi

Adv. Dr.Johnson

July 15 2006

Page 1 of 7
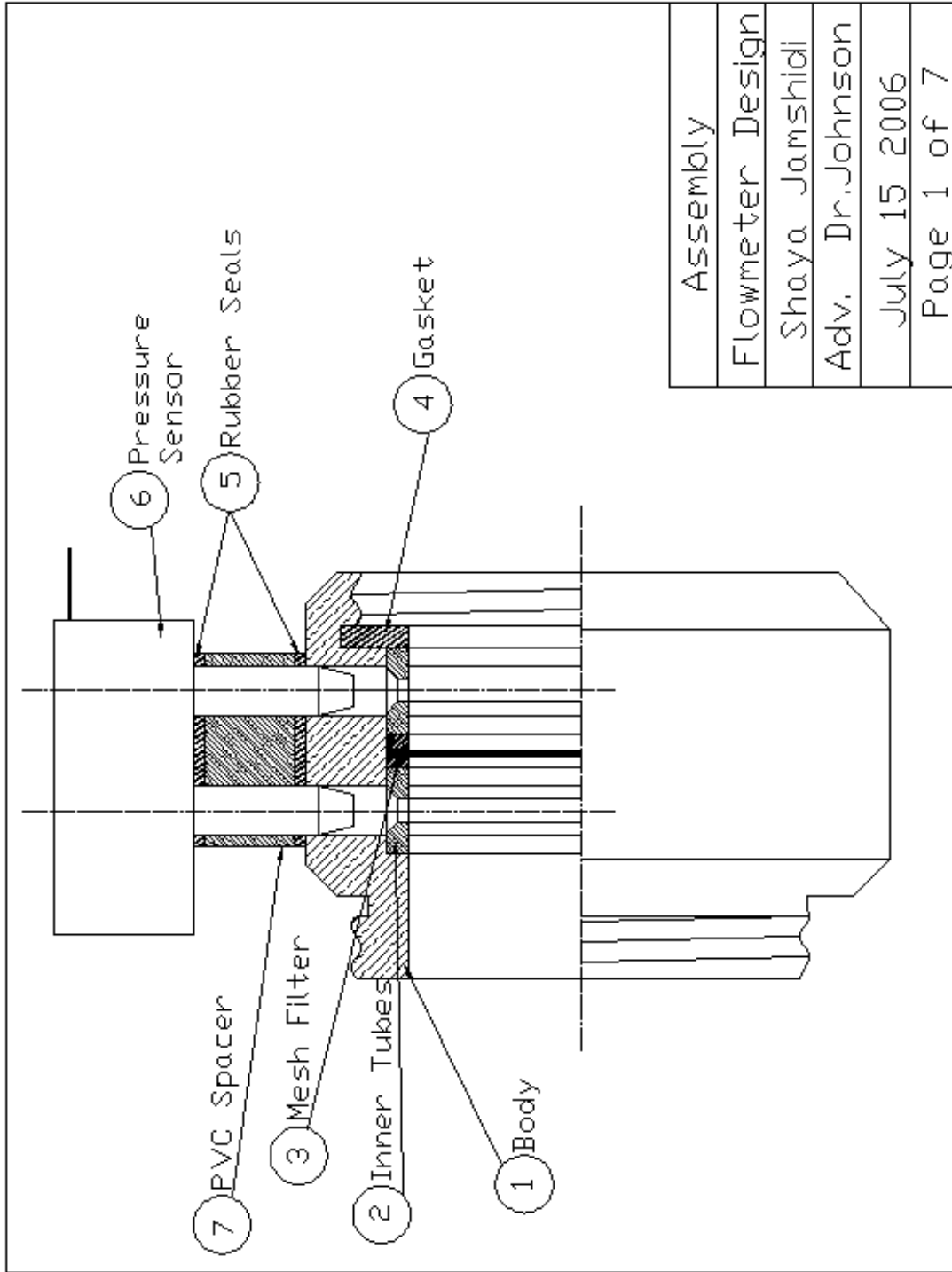
Note: outer surfaces to be knurled
All materials - PVC
All dimensions are in mm
*Inner and outer thread dimensions in FIG 1
Allow for atleast two full pitches
.X = ± .1 mm unless otherwise specified

4 × 45°

ø 51-0 +0.1
ø 48-0 +0.1
ø 44-0 +0.1
ø 34-0 +0.1
ø 30-0 +0.1

2.0
7.0
12.5
23.0
25.0
ø4

ø4.52
ø4.43
31.3
21.6
10.5
ø 54-0 +0.1
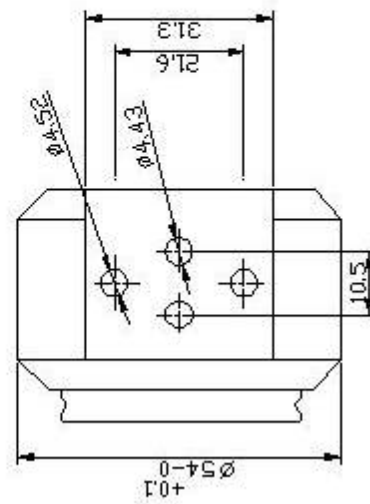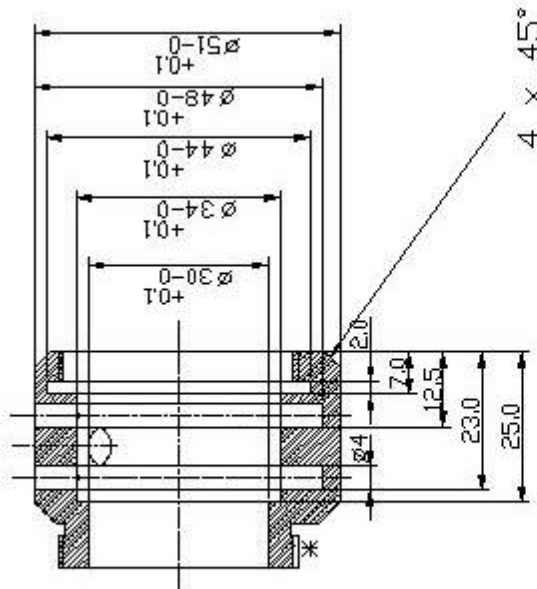
| Main Body |
| Flowmeter Design |
| Shaya Jamshidi |
| Adv. Dr.Johnson |
| July 15 2006 |
| Page 2 of 7 |

2±0.01

7.5 $^{0}_{-0.1}$

Ø30-0.1^{0}

Ø34-0.1^{0}

1mmR X 4:
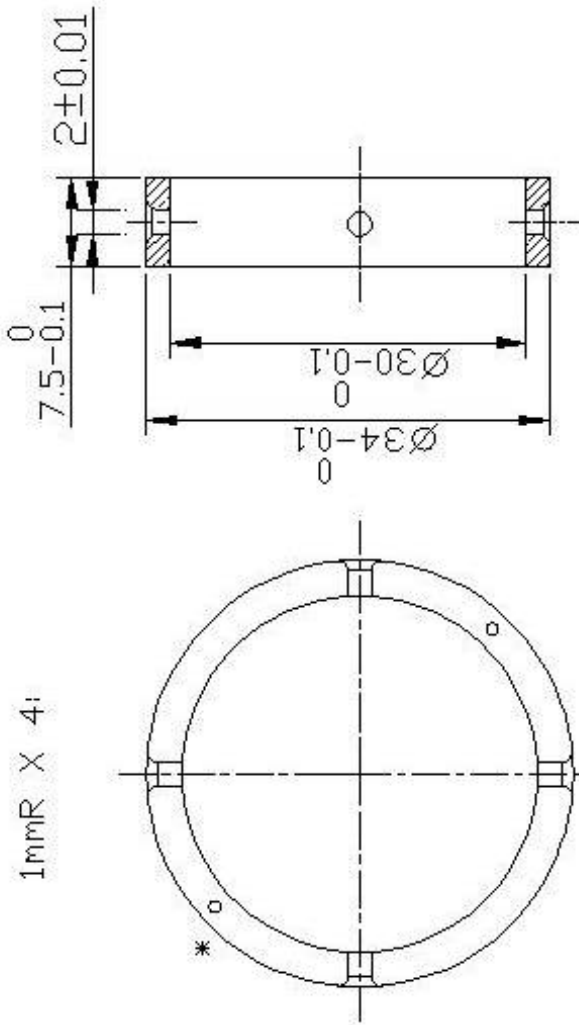
Note:
All materials - PVC
All dimensions are in mm
All filets are .8mm
2 inner tubes needed per design!!
Wholes to be placed for assembly purposes only

| Inner Tubes |
| Flowmeter Design |
| Shaya Jamshidi |
| Adv. Dr.Johnson |
| July 15 2006 |
| Page 3 of 7 |

Mesh Ring-Mounting
Flowmeter Design
Shaya Jamshidi
Adv. Dr.Johnson
July 15 2006
Page 4 of 7

$1.5_{-0.1}^{0}$

$\varnothing 30_{-0.1}^{0}$

$\varnothing 34_{-0.1}^{0}$
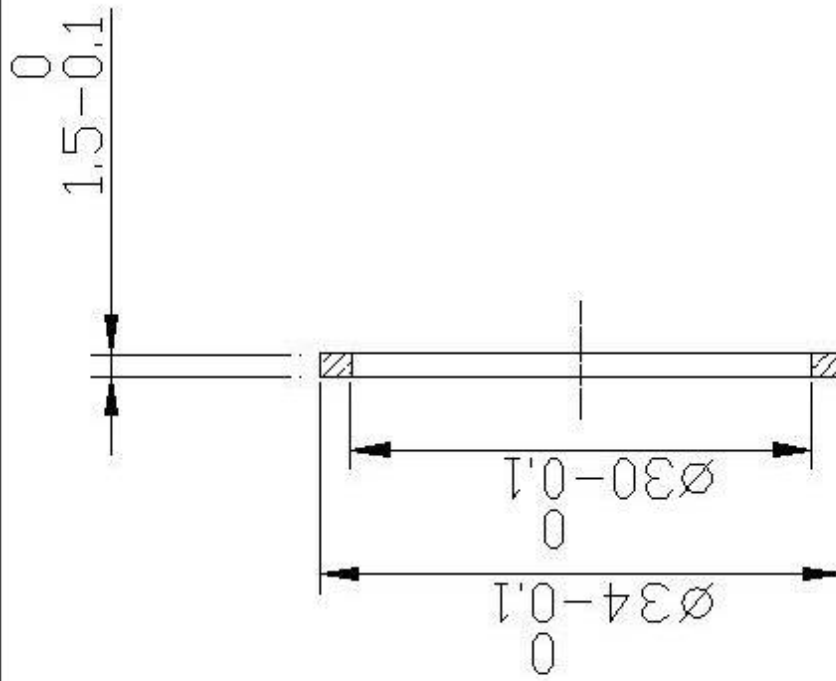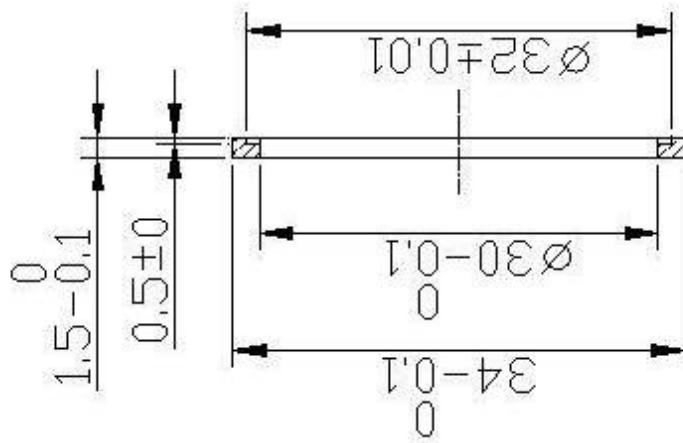
Note:
All materials - PVC
All dimensions are in mm
4 copies needed!!

Mesh Ring-Locking
Flowmeter Design
Shaya Jamshidi
Adv. Dr.Johnson
July 15 2006
Page 5 of 7

Note:
All materials - PVC
All dimensions are in mm
4 copies needed!!

86
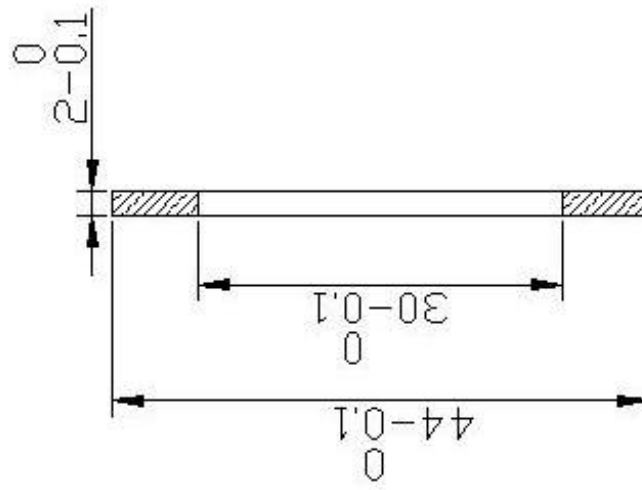
Cross Section

Note:
All materials – Rubber
All dimensions are in mm

Figure 1

NIOSH CBRN Full Facepiece APR Mechanical Connector and Gasket

(Revision 2) 09 Jan 2004

Note: All Dimensions in Millimeters

A External Thread

A
13.72
Minimum
Length of
Effective Thread

40.00 MAX
Rd 40 x 1/7

B
15.00
Minimum
Run-out

Sealing Surface Section Left to the
Choice of the Manufacturer

C Gasket

1.55 Min. (See Note 1)

37.50
Min. Diam.

28.50
Max. Diam.
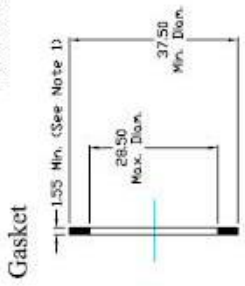
Note:

1. Gasket thickness determined by option B1 or B2 internal thread / sealing gasket.

2. Positive retention of gasket in sealing gland required

3. Right hand threads
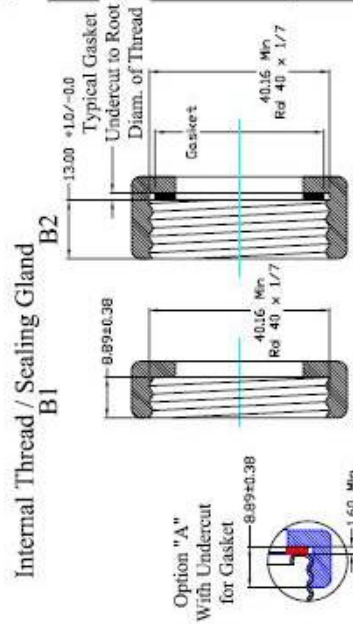
D Dimensions of Threads

Internal Threads
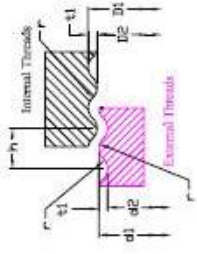
External Threads

Dimensions in millimeters

Thread	Thread limits								Pitch h	Number of threads per 25.4 Z	Thread height t1	Radius r
	External				Internal							
	Major diameter d1		Minor diameter d2		Major diameter D1		Minor diameter D2					
	max	min	max		min		min	max	h	Z	t1	r
Rd 40 x 1/7	40.00	39.70	38.40		40.16		38.56	38.86	3.629	7	0.8	1.225

B Internal Thread / Sealing Gland

B1

8.89±0.38

40.16 Min.
Rd 40 x 1/7

Option "A"
With Undercut
for Gasket

8.89±0.38

1.60 Min.

Typical Undercut to Root
Diam. of Thread

Option "A"   Option A

B2

13.00 +1.0/-0.0

Typical Gasket
Undercut to Root
Diam. of Thread

Gasket

40.16 Min.
Rd 40 x 1/7

Option B

88

Appendix B – Research Protocol

The Detection of Inhalation Flow Using Respiratory Protective Masks

Abstract: A key step in the proper design of respirators, as well as in the regulation of occupational safety, is the determination of inhalation during exercise. A non-invasive portable meter that detects average and peak inhalation is valuable step in obtaining this overall goal. This meter will be attached externally to a military style respirator mask (M-40A1). A study is being developed at the University of Maryland, College Park that is working to achieve this goal. Results from such a study can be used to determine the effectiveness of respirators in protecting individuals during high intensity labor conditions.

Purpose: This project is intended to determine peak and average inhalation values during exercise at a moderate exercise intensity of 80 % VO_{2max}. Exercise at this intensity will be completed once in a controlled laboratory environment, and a final time outside under moderate environmental conditions.

1. Subject Selection:

a) Who will be the subjects, how will you persuade them to participate, and how many do you expect to participate? If you plan to advertise for subjects, please include a copy of the advertisement.

We plan to recruit 10 participants from the University of Maryland, College Park. A portion of this sample will be drawn from a database stored in the Human Performance Laboratory located in the Biological Resources Engineering Department. Additional subjects will be selected through day-to-day interaction within the campus community.

b) Will the subjects be selected for any specific characteristics (e.g. age, sex, race, ethnic origin, religion, or any social or economical qualifications)?

We will be selecting subjects between the ages of 18-40 years.

c) State why the selection will be made on the basis or the bases given in 2(b)?

The selection criteria stipulated in 2(b) reflects a desire to recruit individuals who are at minimal risk while taking part in vigorous physical activities. Vigorous exercise may induce life-threatening cardiovascular responses in older populations with known cardiovascular diseases; therefore, this group may not be ideal for this project. The American College of Sports Medicine (ACSM) in the Guidelines for Exercise Testing and Prescription (6th edition), states that vigorous physical exercise is appropriate for asymptomatic individuals between the ages of 18-40 years, and that medical clearance is not required for this group prior to initiating a vigorous exercise program. This project will not provide medical clearance for prospective participants, and as a result, it is important to select individuals (aged 18-40 years) who do not require medical clearance and are at minimal risk for cardiovascular events while performing vigorous exercise.

2. Describe precisely what will be done to the subject.

Orientation

All participants will be asked to report for a one-hour orientation session. An investigator will be present at this session to explain the test procedures and methods applicable to this project. Volunteers will be provided with a written informed consent document outlining these procedures and methods. Participants will be asked to read and sign this document before being allowed to take part in this study.

Volunteers will be asked to complete several questionnaires. The first questionnaire will be a brief medical history document designed to provide investigators with the individual's present and past health background as related to the study. Next, the subject will be administered a Physical Activity Readiness Questionnaire (PAR-Q) to determine whether exercise is appropriate at this time without first seeking medical clearance. The American College of Sports Medicine, in the Guidelines for Exercise Testing and Prescription, suggests administering this questionnaire to asymptomatic individuals prior to instituting vigorous exercise programs. The medical history and physical activity questionnaires will be used as screening tools to exclude individuals who are at risk for cardiovascular events when performing vigorous physical activities. The Spielberger State-Trait Anxiety Inventory will be the final questionnaire administered to volunteers, providing investigators with information on the individual's present and general anxiety disposition. These questions provide feedback on anxiety and are not intended to diagnose any psychological state.

All participants will be provided the opportunity to have any questions regarding this study answered at this time or throughout the duration of the remaining test sessions.

Maximal Aerobic Capacity

All participants will undergo a maximal oxygen consumption assessment using a Quinton motorized treadmill. First, participants will be allowed to warm-up on the treadmill for approximately 5 minutes at 50-60% of his or her age-predicted maximum heart rate, followed immediately by a brief stretching period. Next, the volunteer will be seated and fitted with a Hans Rudolph breathing mask for the collection of expiratory air. The test will begin with the treadmill speed and grade gradually ramped to the desired work rate (50-60% age-predicted maximum heart rate response) with this moment signifying the initial stage and lasting approximately 3 minutes. At the completion of this stage, a new work rate will be selected and the participant will be required to work at this intensity for another 3 minutes. Work rates will be modified every third minute during the maximal aerobic assessment period. The session will be terminated If the participant fails to display a sufficient rise in oxygen consumption rate (<150 ml/min) to correspond to the new work rate, If the individual reaches his or her age-predicted maximal heart rate, If the individual displays a response that contraindicates continued assessment (e.g. irregular EKG tracings), or If the participant requests that the session be terminated. The maximal aerobic assessment will last approximately 9-15 minutes.

A noninvasive Polar heart rate monitor will be used to assess heart rate responses during the session.

Test Conditions

Participants will be asked to report to the lab on 2 separate days to exercise once on a Quinton motorized treadmill at 80% of their maximal aerobic capacity as determined by VO_{2max}. On the second day, the subject will exercise at roughly this same intensity outdoors, on Ludwig Field/Kehoe Track. Test sessions may or may not be completed on consecutive days, as based on subject availability. Due to the weather conditions, it may be necessary to run some of the tests on consecutive days. All of the test will be done with the subject wearing a military-style respiratory mask with an external flow meter attached. All tests will be run in the same manner, the only difference being that in one test the subject is indoors on a treadmill, or outdoors on a

racetrack.

Test sessions will include warm-up or stretching periods directly prior to commencement of the exercise. This is to ensure that the subject is adequately prepared to exercise for a period without the risk of muscle injury or cardiovascular abnormalities.

After arriving in the Human Performance Lab, subjects will be asked to start walking on a treadmill for roughly five minutes as warm-up. Next they will be asked to stretch their muscles for 5-10 minutes in an attempt to ensure that all their muscles are properly stretched and that they are ready for exercise. The subjects will then be fitted with a M40 military-style negative pressure respiratory mask with the attached external flow meter that has been adjusted for standard conditions (contains the standard filter). The indoor testing condition will be run on a treadmill at 0% grade until volitional fatigue; only the speed of the treadmill belt will be adjusted to elicit the specific work rate desired. The grade will be held constant during the exercise tests for enhanced comparison and result interpretation. The speed of the treadmill will be set to the appropriate level to elicit the specified work rate, and the treadmill will be turned on while the subject is standing over the belt. Once outdoors, the subject will be asked to maintain a particular speed based on previously obtained data from their VO2max. Data logging and timing of the test will initiate once the subject starts moving on belt, or on outdoor racing track. When the subject is no longer able to proceed with the test as based on his or her fatigue level, data logging will stop, the treadmill will be slowed before coming to a stop, and the time duration of the test will be recorded. When outdoors, the subject can voluntarily stop moving as they please. It is important to note that for all exercise tests, a short five minute cool-down period will follow completion of the test to ensure subject safety and return to physical control.

A Polar heart rate monitor will be used to provide heart rate responses during the exercise sessions. Rating of Perceived Exertion and Breathing Apparatus Comfort scales will be taken periodically during each test to provide investigators with subjective feedback regarding the independent variables (e.g. exercise intensity and subject-perceived mask comfort). Tests will be run at approximately the same time of day in an attempt to ensure that physiological conditions are constant and any diurnal cycles are not influencing the results obtained. All of the procedures listed above will

be employed for all exercise test sessions, namely all respiratory mask conditions (with or without) and at all exercise intensities.

At 80% VO_{2max} exercise intensities, it is anticipated that exercise will last approximately 15-20 minutes. A single test condition, including the preparation time will last up to approximately 30-45 minutes; therefore, this project will necessitate that individuals commit roughly 2 hours to fulfill the requirements (1 orientation session with a maximal aerobic capacity test and 2 test conditions) outlined in this study. Participants are free to withdraw from this project at anytime without incurring a penalty. This request may be expressed to an investigator through verbal or written communication.

3. Risks and Benefits: Are there any risks to the subjects? If so, what are these risks? What potential benefits will accrue to justify taking these risks?

Risks

Vigorous physical exercise may produce undesired cardiovascular responses in at-risk populations, leading to possibly life-threatening situations. The medical history and physical activity questionnaires will be used as screening tools to exclude this at-risk group. An Automated External Defibrillator (AED) will be available for use should a cardiovascular incident arise during test sessions. Investigators are trained and certified in the use of the AED.

Benefits

Participants will not receive monetary benefits from taking part in this study; however, individuals will be provided with test results upon completion of this project.

Confidentiality

All participants will be assigned an identification number and will be referred to by this descriptor in any presentation or publication of test findings. All files will be stored and maintained in the assistant investigator's office with access permitted to only those individuals directly responsible for the collection and analysis of test data.

Information and Consent Form

An investigator will meet with each participant to explain the test procedures and methods applicable to this project prior to the test date. The participant will be provided with a written informed consent document outlining these procedures and

methods. Volunteers will be asked to read and sign this document before being allowed to participate in the investigation.

Conflict of Interest

Investigators do not have a conflict of interest in this project.

HIPPA Compliance

This investigation will not be using protected health information. Identification numbers will be assigned to help ensure the patient's anonymity. Investigators plan to adhere to the guidelines outlined by the University of Maryland at College Park regarding any sensitive information.

Research Outside of the United States

a) Did the investigators previously conduct research in the country where the research will take place? Briefly describe the Investigators' knowledge and experience working with the study population.

Not applicable. All research is taking place in the United States.

b) Are there any regulations, rules or policies for human subjects research in the country where the research will take place? If so, please describe and explain how you will comply with the local human subject protection requirements.

Not applicable. All research is taking place in the United States.

c) Do you anticipate any risks to the research participants in the country where the research will take place, taking into account the population involved, the geographic location, and the culture? If so, please describe. Risks could include physical, psychological, social or economic risks. Do you anticipate that subjects who participate in this research will be placed at risk of criminal or civil liability? If so, please describe.

Not applicable. All research is taking place in the United States.

Research Involving Prisoners

Not applicable. All research is being done using subjects from the University of Maryland population and will not include prisoners.

Appendix C – Physical Activity Readiness Questionnaire

PAR-Q is designed to help you help yourself. Many health benefits are associated with regular exercise, and the completion of PAR-Q is a sensible first step to take If you are planning to increase the amount of physical activity in your life.

For most people, physical activity should not pose any problems or hazard. PAR-Q has been designed to identify the small number of adults for whom physical activity might be inappropriate or those who should have medical advise concerning the type of activity most suitable for them.

Common sense is your best guide in answering these few questions. Please read the carefully and check **YES** or **NO** opposite the question If it applies to you. If yes, please explain.

<u>**YES**</u>   <u>**NO**</u>

____ ____   1.   Has your doctor ever said you have heart trouble?

 Yes, _____

____ ____   2.   Do you frequently have pains in your heart and chest?

 Yes, _____

____ ____   3.   Do you often feel fain or have spells of severe dizziness?

 Yes, _____

____ ____   4.   Has a doctor ever said your blood pressure was too high?

 Yes, _____

____ ____   5.   Has your doctor ever told you that you have a bone or joint problem(s), such as arthritis that has been aggravated by exercise, or might be made worse with exercise?

 Yes, _____

____ ____   6.   Is there a good physical reason, not mentioned here, why you should not follow an activity program even If you wanted to?

 Yes, _____

____ ____   7.   Are you over age 60 **<u>and</u>** not accustomed to vigorous exercise?

 Yes, _____

____ ____   8.   Do you suffer from any problems of the lower back, i.e., chronic pain, or numbness?

 Yes, _____

____ ____ 9. Are you currently taking any medications? If YES, please specify.

Yes, _____

____ ____ 10. Do you currently have a disability or a communicable disease? If YES,

Please specify,

Yes, _____

If you answered NO to all questions above, it gives a general indication that you may participate in physical and aerobic fitness activities and/or fitness evaluation testing. The fact that you answered NO to the above questions, is no guarantee that you will have a normal response to exercise. If you answered Yes to any of the above questions, then you may need written permission from a physician before participating in physical and aerobic fitness activities and/or fitness evaluation testing at the Deneka Fitness Center.

_____   _____   _____

Print Name   Signature   Date

Please Note: If you contract a communicable disease, it is your responsibility to inform the staff of the Clarkson University Fitness Center of this condition and your membership may be suspended until this condition is cured or in a state of remission.

Appendix D – Program Code

Front Panel
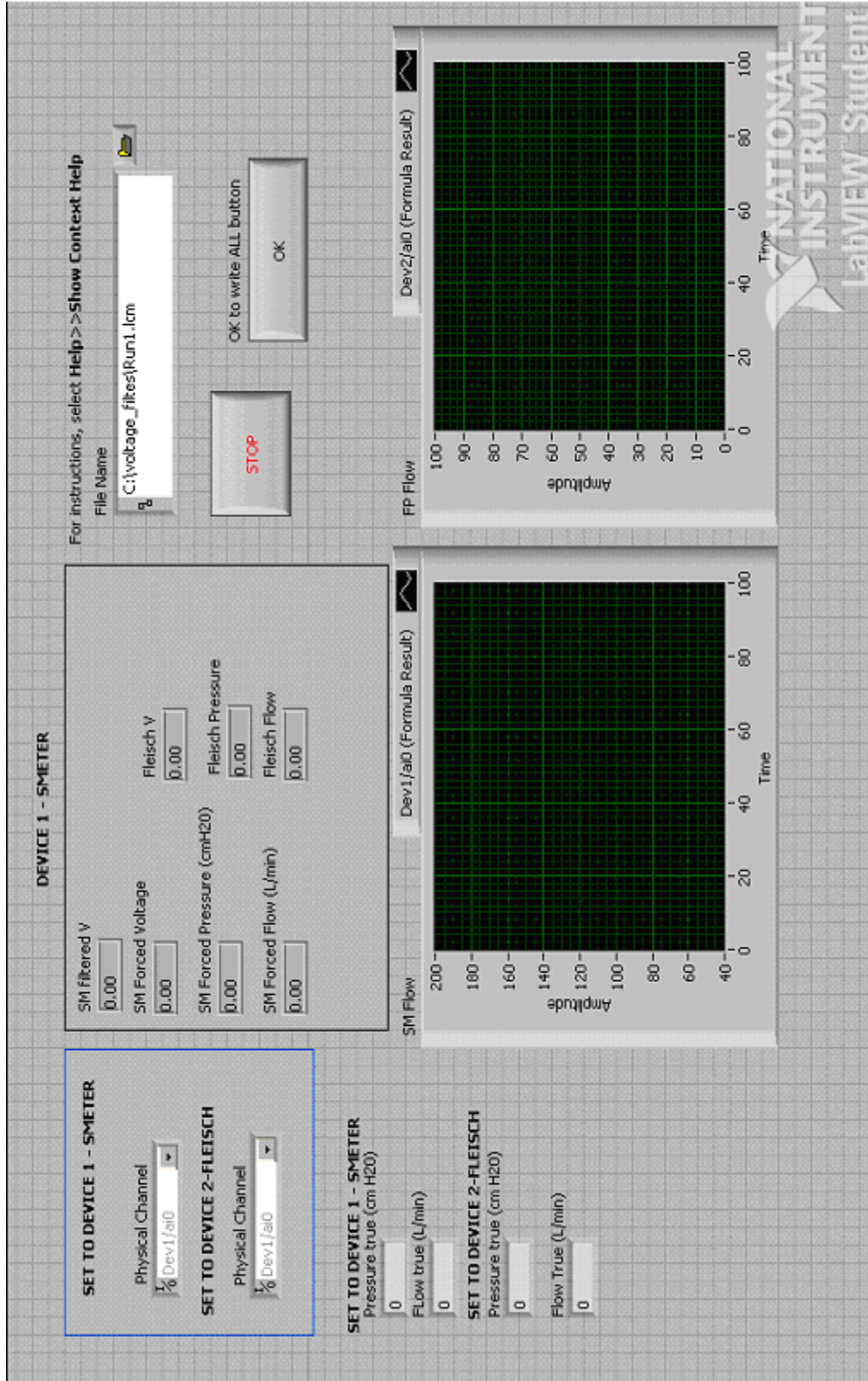
Block Diagram
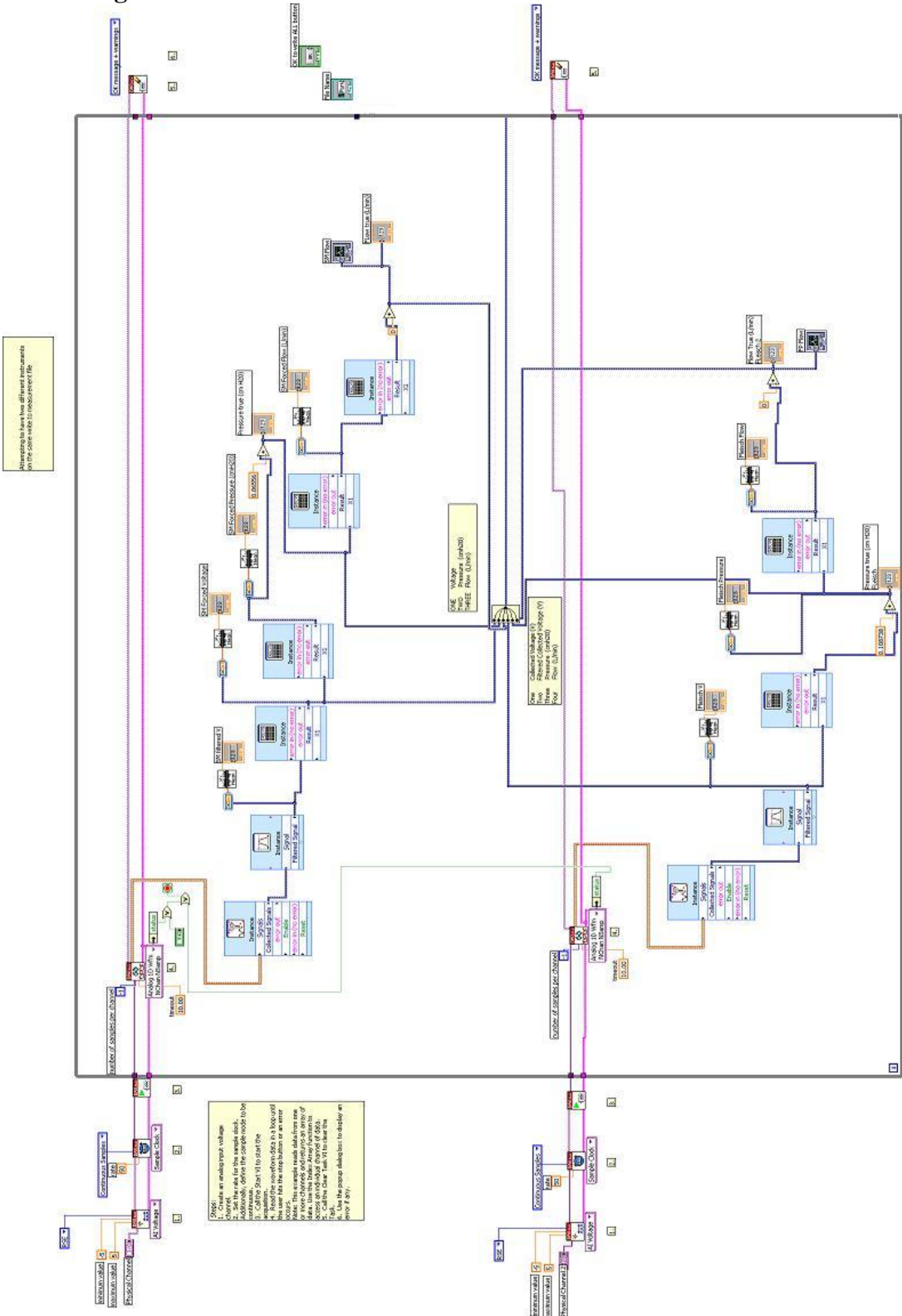
Appendix E – Pressure Sensor Specifications Sheet

Amplified Low Pressure Sensors

1 mbar (0.4 In H2O) to 30 In H2O Pressure Sensors

Features

- 0 to 1 mbar to 0 to 30 In H2O Pressure Ranges
- Ratiometric 4V Output
- Temperature Compensated
- Calibrated Zero and Span

Applications

- Medical Instrumentation
- Environmental Controls
- HVAC

General Description

The Amplified line of low pressure sensors is based upon a proprietary technology to reduce all output offset or common mode errors. This model provides a ratiometric 4-volt output with superior output offset characteristics. Output offset errors due to change in temperature, stability to warm-up, stability to long time period, and position sensitivity are all significantly reduced when compared to conventional compensation methods. In addition the sensor utilizes a silicon, micromachined, stress concentration enhanced structure to provide a very linear output to measured pressure.

These calibrated and temperature compensated sensors give an accurate and stable output over a wide temperature range. This series is intended for use with non-corrosive, non-ionic working fluids such as air, dry gases and the like.

The output of the device is ratiometric to the supply voltage over a supply voltage range of 4.5 to 5.5 volts.

Physical Dimensions
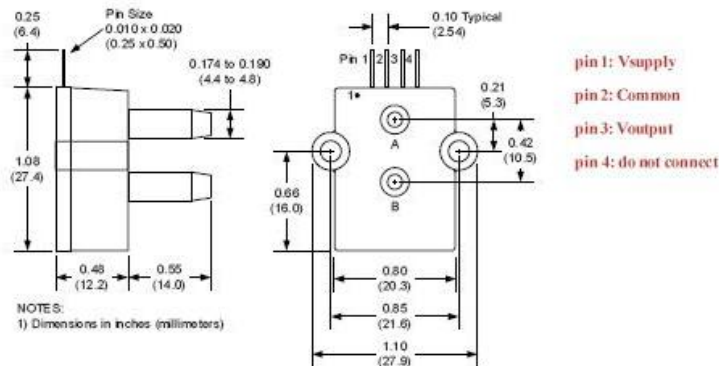
0.25 (6.4)
Pin Size 0.010 x 0.020 (0.25 x 0.50)
0.174 to 0.190 (4.4 to 4.8)
0.10 Typical (2.54)
Pin 1 2 3 4
0.21 (5.3)
1.08 (27.4)
0.42 (10.5)
A
0.66 (16.0)
B
0.48 (12.2)
0.55 (14.0)
0.80 (20.3)
0.85 (21.6)
1.10 (27.9)

pin 1: Vsupply
pin 2: Common
pin 3: Voutput
pin 4: do not connect

NOTES:
1) Dimensions in inches (millimeters)

All Sensors

Pressure Sensor Ratings

Supply Supply Voltage VS	+4.5 to +5.5 Vdc
Common-mode pressure	-10 to +10 psig
Lead Temperature, max (soldering 2-4 sec.)	250°C

Environmental Specifications

Temperature Ranges	
Compensated	5 to 50° C
Operating	-25 to 85° C
Storage	-40 to 125° C
Humidity Limits	0 to 95% RH
	(non condensing)

Standard Pressure Ranges

Part Number	Operating Pressure	Nominal Span	Proof Pressure	Burst Pressure
1 MBAR-D-4V	±1 mbar	4 V	100 In H2O	200 In H2O
1 INCH-D-4V	±1 In H2O	4 V	100 In H2O	200 In H2O
1 INCH-G-4V	0 - 1 In H2O	4 V	100 In H2O	200 In H2O
2.5 INCH-D-4V	±2.5 In H2O	4 V	200 In H2O	300 In H2O
5 INCH-D-4V	± 5 In H2O	4 V	200 In H2O	300 In H2O
5 INCH-G-4V	0 - 5 In H2O	4 V	200 In H2O	300 In H2O
10 INCH-D-4V	±10 In H2O	4 V	200 In H2O	300 In H2O
10 INCH-G-4V	0 - 10 In H2O	4 V	200 In H2O	300 In H2O
20 INCH-D-4V	±20 In H2O	4 V	300 In H2O	500 In H2O
20 INCH-G-4V	0 - 20 In H2O	4 V	300 In H2O	500 In H2O
30 INCH-D-4V	±30 In H2O	4 V	500 In H2O	800 In H2O
30 INCH-G-4V	0 - 30 In H2O		500 In H2O	800 In H2O

Performance Characteristics for: 1 MBAR-D-4V

Parameter, NOTE 1	Minimum	Nominal	Maximum	Units
Operating Range, differential pressure		±1.0		mbar
Output Span, NOTE 5	±1.80	±2.0	±2.20	volt
Offset Voltage @ zero differential pressure	2.00	2.25	2.50	volt
Offset Temperature Shift (5°C-50°C), NOTE 2			±120	mvolt
Offset Warm-up Shift, NOTE 3		±20		mvolt
Offset Position Sensitivity (±1g)		±40		mvolt
Offset Long Term Drift (one year)		±20		mvolt
Linearity, hysteresis error, NOTE 4		0.05	0.25	%fs
Span Shift (5°C-50°C), NOTE 2			±4	%span

Amplified Low Pressure Sensors

Appendix F – USB6009 Specifications Sheet

Low-Cost, Bus-Powered Multifunction DAQ for USB – 12- or 14-Bit, up to 48 kS/s, 8 Analog Inputs

NI USB-6008, NI USB-6009

- 8 analog inputs at 12 or 14 bits, up to 48 kS/s
- 2 analog outputs at 12 bits, software-timed
- 12 TTL/CMOS digital I/O lines
- 32-bit, 5 MHz counter
- Digital triggering
- Bus-powered
- 1-year warranty

Operating Systems
- Windows Vista (32- and 64-bit)/XP/2000
- Mac OS X[1]
- Linux[1]
- Windows Mobile[1]
- Windows CE[1]

Recommended Software
- LabVIEW
- LabVIEW SignalExpress
- LabWindows™/CVI
- Measurement Studio

Other Compatible Software
- C#, Visual Basic .NET
- ANSI C/C++

Measurement Services Software (included)
- NI-DAQmx driver software
- Measurement & Automation Explorer configuration utility
- LabVIEW SignalExpress LE

[1]You need to download NI-DAQmx Base for these operating systems.

Product	Bus	Analog Inputs[1]	Input Resolution (bits)	Max Sampling Rate (kS/s)	Input Range (V)	Analog Outputs	Output Resolution (bits)	Output Rate (Hz)	Output Range (V)	Digital I/O Lines	32-Bit Counter	Trigger
USB-6009	USB	8 SE/4 DI	14	48	±1 to ±20	2	12	150	0 to 5	12	1	Digital
USB-6008	USB	8 SE/4 DI	12	10	±1 to ±20	2	12	150	0 to 5	12	1	Digital

[1]SE = single ended, DI = differential   [2]Software-timed

Overview and Applications

With recent bandwidth improvements and new innovations from National Instruments, USB has evolved into a core bus of choice for measurement applications. The NI USB-6008 and USB-6009 are low-cost entry points to NI flagship data acquisition (DAQ) devices. With plug-and-play USB connectivity, these modules are simple enough for quick measurements but versatile enough for more complex measurement applications.

The USB-6008 and USB-6009 are ideal for a number of applications where low cost, small form factor, and simplicity are essential. Examples include:

- Data logging – quick and easy environmental or voltage data logging
- Academic lab use – student ownership of DAQ hardware for completely interactive lab-based courses (Academic pricing available. Visit ni.com/academic for details.)
- OEM applications as I/O for embedded systems

Recommended Software

National Instruments measurement services software, built around NI-DAQmx driver software, includes intuitive application programming interfaces, configuration tools, I/O assistants, and other tools designed to reduce system setup, configuration, and development time. National Instruments recommends using the latest version of NI-DAQmx driver software for application development in NI LabVIEW, LabVIEW SignalExpress, LabWindows/CVI, and Measurement Studio software. To obtain the latest version of NI-DAQmx, visit ni.com/support/daq/versions.

NI measurement services software speeds up your development with features including:

- A guide to create fast and accurate measurements with no programming using the DAQ Assistant.
- Automatic code generation to create your application in LabVIEW.
- LabWindows/CVI; LabVIEW SignalExpress; and C#, Visual Studio .NET, ANSI C/C++, or Visual Basic using Measurement Studio.
- Multithreaded streaming technology for 1,000 times performance improvements.
- Automatic timing, triggering, and synchronization routing to make advanced applications easy.
- More than 3,000 free software downloads available at ni.com/zone to jump-start your project.
- Software configuration of all digital I/O features without hardware switches/jumpers.
- Single programming interface for analog input, analog output, digital I/O, and counters on hundreds of multifunction DAQ hardware devices. M Series devices are compatible with the following versions (or later) of NI application software – LabVIEW, LabWindows/CVI, or Measurement Studio versions 7.x; and LabVIEW SignalExpress 2.x.

NATIONAL INSTRUMENTS

I/O Connector

Figure 3 shows the USB-6008/6009 OEM device I/O connector pinout. AI signal names are shown in single-ended mode. Differential mode signal names are in parentheses.

+5 V	34	33	PFI 0
D GND	32	31	P1.3
P1.2	30	29	P1.1
P1.0	28	27	P0.7
P0.6	26	25	P0.5
P0.4	24	23	P0.3
P0.2	22	21	P0.1
P0.0	20	19	D GND
LED	18	17	D+
VBUS	16	15	D–
AI GND	14	13	AI GND
AI 4 (AI 0–)	12	11	AI 0 (AI 0+)
AI 5 (AI 1–)	10	9	AI 1 (AI 1+)
AI 6 (AI 2–)	8	7	AI 2 (AI 2+)
AI 7 (AI 3–)	6	5	AI 3 (AI 3+)
AI GND	4	3	AI GND
AO 1	2	1	AO 0

Figure 3. USB-6008/6009 OEM Terminal Assignments

Appendix G – User Manual

Calibration Technique:

1. Connect Mask Flow Meter (MFM) (labeled 1) to the M40A1 respirator mask and C2A1 filter.
2. Connect pressure transducer (labeled 2) to MFM body with the screws provided.
3. Connect blue wire (labeled 3) to pressure traducer via the grey connecter (labeled 4) ports highlighted.
4. Secure connector to wire with grey clip provided (labeled 5).
5. Connect wires to USB6009 (labeled 6).
6. Connect USB6009 to computer via a Universal Serial Bus (USB) port.
7. Place M40A1 mask to head form of breathing machine for dynamic data calibration.
8. Set the parameters of the breathing machine to Profile of 3, Amplitude of 100.
9. Turn on the breathing machine and allow the machine to remain on for five minutes prior to starting the simulated breathing cycles.
10. Turn on Computer
11. If you are using other programs, close all unrelated programs.
12. Select "MFM program" from program list and allow LabVIEW Program to operate.
13. If physical channels are different from 0, please select physical channel.
14. If voltage input is different from $\pm$ 5V, then set appropriate voltage range.
15. If sample rate is different from 50Hz, then set sample rate.
16. If sample mode is desired to be different from continuous, then set sample mode.
17. If set sample scan mode is different from continuous, set sample scan mode.
18. If filtration mode is different from "smoothing", set filtration mode.
19. Set file name path as desired.
20. Click on "run" to initiate the program.
21. Allow data to accumulate for thirty seconds.
22. Observe data on "Flow" chart.
23. Press "Stop" at anytime to terminate program.
24. Open Microsoft Excel program.
25. Open the file of data, saved in the location specified under file path name.
26. When the dialogue box opens, select "Finish" and the file path name will open. Note: if the number 54728 data points, the duration of exercise time must be saved under different file names to avoid truncation of data points.

27. Manipulate the data as needed, noting that the data is stored in separate columns. Relative time is plotted in column one with units of seconds. Voltage is plotted on the second column with units of Volts. Flow is plotted in the second column with units of L/min.
28. Compare the voltage values observed from "standard" flow to the provided set of values (labeled calibration data).
29. Plot the standard voltage values, x values, from calibration procedure against the "standard" flow values, y values, in an excel chart.
30. Click on a data point, and select "add trend line" and select a "polynomial" trend line with an order of 3.
31. Under the options tab, select display equation on chart. This will be the new calibration equation.
32. Select the MFM program block diagram. Select "Formula" icon and insert the calibration equation.
33. Save the program file. It is now ready for usage.
34. Calibrate the MFM system per ASTM
35. If any errors arise at any time, observe the error number, and determine the error code at the National Instruments website www.ni.com.

User Manual Technique:
1. Connect Mask Flow Meter (MFM) (labeled 1) to the M40A1 respirator mask and C2A1 filter.
2. Connect pressure transducer (labeled 2) to MFM body with the screws provided.
3. Connect blue wire (labeled 3) to pressure traducer via the grey connecter (labeled 4) ports highlighted.
4. Secure connector to wire with grey clip provided (labeled 5).
5. Connect wires to USB6009 (labeled 6).
6. Connect USB6009 to computer via a Universal Serial Bus (USB) port.
7. Turn on Computer
8. If you are using other programs, close all unrelated programs.
9. Select "MFM program" from program list and allow LabVIEW Program to operate.
10. If physical channels are different from 0, please select physical channel.
11. If voltage input is different from $\pm$ 5V, then set appropriate voltage range.

12. If sample rate is different from 50Hz, then set sample rate.
13. If sample mode is desired to be different from continuous, then set sample mode.
14. If set sample scan mode is different from continuous, set sample scan mode.
15. If filtration mode is different from "smoothing", set filtration mode.
16. Set file name path as desired.
17. Click on "run" to initiate the program.
18. Observe data on "Flow" chart.
19. Press "Stop" at anytime to terminate program.
20. Close LabVIEW program.
21. Open Microsoft Excel program.
22. Open the file of data, saved in the location specified under file path name.
23. When the dialogue box opens, select "Finish" and the file path name will open. Note: if the number 54728 data points, the duration of exercise time must be saved under different file names to avoid truncation of data points.
24. Manipulate the data as needed, noting that the data is stored in separate columns. Relative time is plotted in column one. Flow is plotted in the second column.
25. If any errors arise at any time, observe the error number, and determine the error code at the National Instruments website www.ni.com.

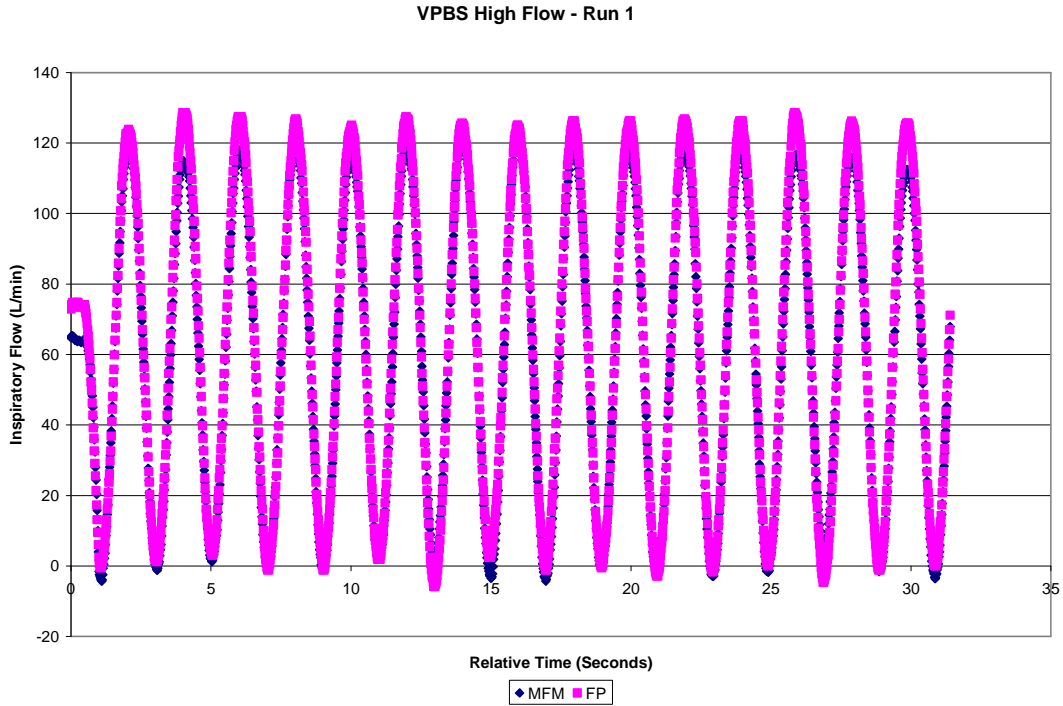# Appendix H – VPBS Testing at Low and High Flow Rates

Sample VPBS Instantaneous Flow versus Time:

VPBS High Flow - Run 1

Sample Data:

Breathing Machine RUN1			
Low Flow Rate			
	MFM		**FP**	
Breath	VI_{avg}	PIF	VI_{avg}	PIF
1	36.168	65.518	33.057	65.225
2	34.287	65.895	35.466	67
3	33.502	67.051	35.596	68.776
4	36.701	65.846	34.384	65.816
5	36.998	67.831	36.846	68.776
6	36.9	67.718	36.579	68.184
7	35.958	65.302	34.645	65.225
8	33.725	65.307	35.081	66.408
9	33.919	66.069	37.195	68.184
10	34.399	66.112	36.253	67
11	35.058	65.895	35.507	67

Breathing Machine RUN1		
T-test Results for Average Inspiratory Flow		
t-Test: Two-Sample Assuming Unequal Variances		
	Variable 1	Variable 2
Mean	35.651809	35.478962
Variance	1.8387935	1.4362801
Observations	30	30
Hypothesized Mean Difference	0	
df	57	
t Stat	0.5231333	
P(T<=t) one-tail	0.3014546	
t Critical one-tail	1.6720289	
P(T<=t) two-tail	0.6029093	
t Critical two-tail	2.0024654	

12	38.298	66.561	35.847	66.408
13	36.581	64.171	35.644	64.041
14	37.181	67.658	37.443	68.776
15	34.461	67.094	35.249	68.776
16	33.902	65.677	35.081	67
17	36.954	65.216	33.631	65.225
18	35.574	65.067	33.827	65.816
19	37.543	66.104	35.212	65.816
20	36.85	66.112	36.411	67
21	35.756	64.904	34.843	64.041
22	36.406	67.546	37.24	68.184
23	36.311	65.017	33.008	64.633
24	36.059	64.783	34.747	65.225
25	35.963	66.519	35.673	66.408
26	35.462	64.148	37.492	65.816
27	35.36	66.873	36.183	67.592
28	33.624	65.634	36.188	67
29	36.423	63.431	34.765	64.041
30	33.229	64.324	35.277	65.816
average	35.652	65.846	35.479	66.507

t-Test: Two-Sample Assuming Unequal Variances

	Variable 1	Variable 2
Mean	65.846121	66.506959
Variance	1.2838078	2.152102
Observations	30	30
Hypothesized Mean Difference	0	
df	55	
t Stat	-1.952696	
P(T<=t) one-tail	0.0279761	
t Critical one-tail	1.673034	
P(T<=t) two-tail	0.0559522	
t Critical two-tail	2.0040448	

Breathing Machine RUN2			
Low Flow Rate			
	MFM		FP	
Breath	Vlavg	PIF	Vlavg	PIF
1	37.274	66.654	35.656	66.408
2	34.203	65.68	34.207	67
3	35.121	63.43	35.408	64.041
4	34.53	65.635	34.744	65.816
5	35.944	66.263	35.963	67
6	35.353	65.75	34.952	65.816
7	35.455	65.992	34.022	65.225

t-Test: Two-Sample Assuming Unequal Variances

	Variable 1	Variable 2
Mean	35.61133	35.14334
Variance	1.930656	1.892498
Observations	29	29
Hypothesized Mean Difference	0	

8	35.984	66.783	36.326	67	df	56	
9	35.166	66.108	35.925	66.408	t Stat	1.288911	
10	35.126	65.171	35.602	65.816	P(T<=t) one-tail	0.101364	
11	34.908	65.635	34.436	65.816	t Critical one-tail	1.672522	
12	35.459	66.783	34.699	67	P(T<=t) two-tail	0.202728	
13	34.62	65.287	34.807	65.816	t Critical two-tail	2.003241	
14	33.923	61.063	32.442	61.082			
15	34.814	64.457	31.993	63.449	T-test Results for PIF		
16	33.753	65.964	33.264	66.408	t-Test: Two-Sample Assuming Unequal Variances		
17	36.01	65.935	36.389	66.408			
							Variable
18	38.377	63.925	37.873	64.041		*Variable 1*	*2*
19	39.152	66.453	37.967	66.408	Mean	65.52474	65.77564
20	37.992	65.606	36.77	65.816	Variance	1.805052	2.150089
21	35.789	64.959	34.799	65.225	Observations	29	29
22	37.101	65.663	35.912	65.816	Hypothesized Mean Difference	0	
23	35.371	63.741	33.677	63.449	df	56	
24	35.311	64.988	34.953	65.225	t Stat	-0.67938	
25	36.379	67.787	35.668	68.184	P(T<=t) one-tail	0.249847	
26	37.204	67.285	36.667	67.592	t Critical one-tail	1.672522	
27	33.49	64.26	34.943	65.225	P(T<=t) two-tail	0.499695	
28	34.454	66.61	34.56	67	t Critical two-tail	2.003241	
29	34.465	66.35	34.532	67			
average	35.611	65.525	35.143	65.776			

Appendix I – Subject Testing at Rest and at 85% of Age Predicted Maximum Heart Rate Work Loads

Sample VPBS Instantaneous Flow versus Time:

Subject #1 - At Rest
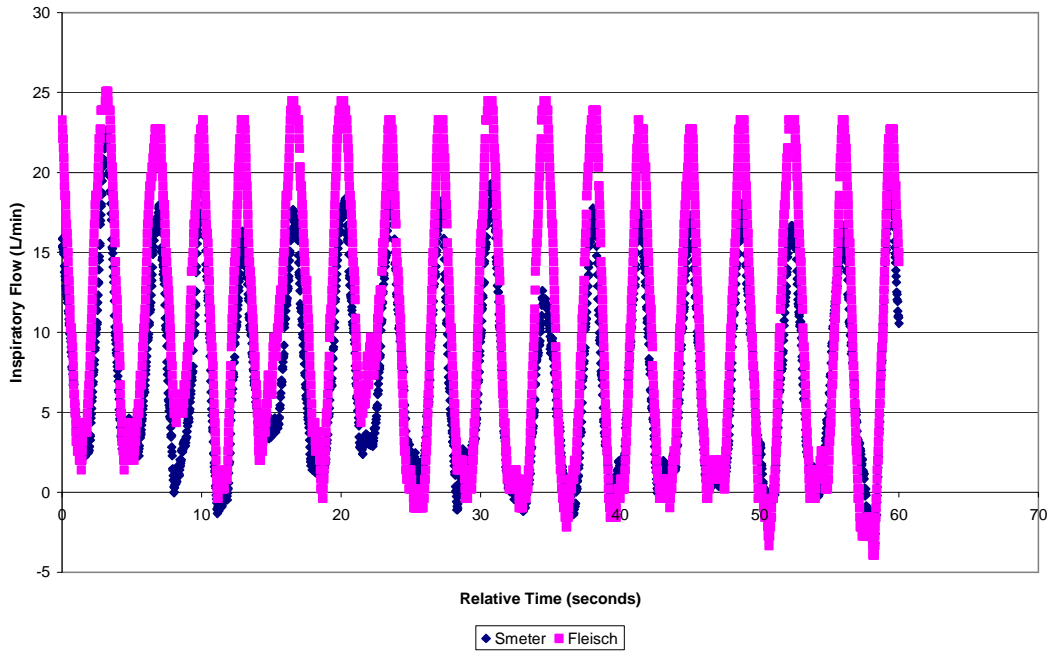
Subject 1 - At Work Load of 85% Age Predicted Maximum Heart Rate

Sample Data:

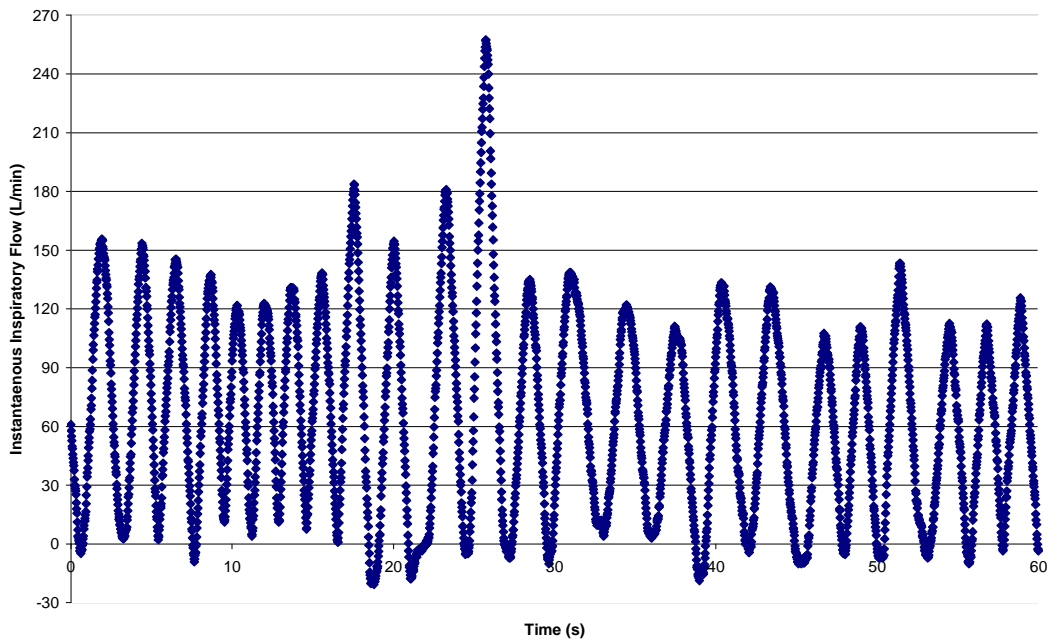| Subject 1 At 85% Maximum Heart Rate		
Breath	VI avg	PIF
1	72.1872126	155.578153
2	77.7378253	152.460845
3	74.813698	145.528962
4	73.0688525	137.539294
5	71.2072288	121.795883
6	71.6079451	122.85178
7	81.7490635	130.91446
8	75.1344699	138.235163
9	91.756317	183.729311
10	55.9311488	154.539099
11	59.1239245	179.187195
12	107.761682	254.029442
13	63.7480195	135.10169
14	75.3363973	138.235163
15	52.4546657	111.170653
16	57.498847	133.3584
17	56.0155989	131.263848
18	46.651269	107.598227
19	55.5888319	110.814165
20	55.2941522	142.058347
21	51.6263801	112.594993
22	54.4241731	112.239146
23	59.7348091	125.662434
average	66.9761961	140.716811

Subject 1 At Rest				
	MFM		**FP**	
Breath	VI avg	PIF	Vi avg	PIF
1	12.604502	23.05783	13.512692	25.068351
2	10.764166	20.875121	11.561538	22.70092
3	11.573586	21.421922	12.419015	23.292778
4	9.8034781	21.783376	10.525008	23.68735
5	10.696072	22.139372	11.497902	24.081921
6	13.717211	22.504547	14.721643	24.476493
7	8.0448977	21.420201	8.6115671	23.292778
8	9.9053563	21.419228	10.624674	23.292778
9	8.5534122	22.507935	9.1647546	24.476493
10	9.0299149	22.492757	9.7218316	24.476493
11	10.622809	21.959266	11.419142	23.884636
12	8.5320633	20.872966	9.1398113	22.70092
13	7.7657969	20.873204	8.3191154	22.70092
14	6.7995825	21.422861	7.280486	23.297
15	9.9766927	21.414939	10.708586	23.292778
16	5.6804059	21.417951	6.0619052	23.294778
average	9.6293716	21.723967	10.330604	23.626087

Subject 2 At 85% Maximum Heart Rate		
Breath	Viavg	PIF
1	55.353412	121.66938
2	53.839175	114.03458
3	48.095401	114.03458
4	43.566587	109.85796
5	50.386164	125.86688
6	60.140784	136.07012
7	54.013187	123.378
8	60.027938	124.9067
9	63.652406	132.49326
10	68.766208	136.07012
11	62.800452	126.05936
12	60.5704	126.44474
13	53.887085	119.59708
14	55.730754	125.09844
15	55.229074	134.87253
16	60.462639	133.87859
17	56.561132	122.23761
18	57.930139	126.63766
19	56.075429	121.10246
20	57.400152	118.101
21	56.88655	126.44474
22	57.579591	124.52365
average	56.770666	124.69907

Subject 2 At Rest				
	Prototype		Fleisch	
Breath	VI avg	PIF	VI avg	PIF
1	5.6038943	11.769323	5.2031033	12.829692
2	5.4551764	5.8250132	5.2989642	6.3357878
3	5.9998042	8.836987	5.8305494	9.739318
4	5.8977365	7.4712499	5.7082806	8.1635858
5	6.1589868	10.985016	5.7755635	11.943145
6	5.0571263	7.4162663	4.8384364	8.0874803
7	4.3098313	5.6821563	4.1302447	6.1730807
8	5.7724151	9.7845293	5.5079292	10.717409
9	6.6734282	13.837132	6.2280314	15.110677
10	5.8674961	10.607402	5.5385177	11.58047
11	6.0589098	11.061404	5.655326	12.009925
12	5.0418496	6.9806263	4.8590841	7.6317529
13	1.1288369	2.0069262	1.1259066	2.2568084
14	5.4876899	8.8447832	5.2173933	9.6470829
15	4.8052615	5.9692219	4.623707	6.4865527
average	5.2878962	8.4718691	5.0360692	9.2475179

Bibliography

American Thoracic Society. 1995. Standardization of Spirometry. *American journal of Respiratory & Critical Care Medicine* 152: 1107-1136.

Babb, T., Tuner, N., Saupe, K., and Pawelczyk, J. 1989. Physical Performance During Combinations of Hypercapnic, Resistive and Hot-air Breathing. *American Industrial Hygiene Association Journal* 50:105-111.

Baker, R. 1988. *An Introductory Guide to Flow Measurement.* Oxford: Alden Press.

Beckwith, T., Buck, NL and Morgan, R. 1982. *Mechanical Measurement Third Edition.* Redding: Addison Wesley Publishing Co.

Benchetrit, G. 2000. Breathing Pattern in Humans: Diversity and Individuality. *Respiratory Physiology* 123-129.

Berndtsson, G. 2003. A New Simplified Technique for Measuring Inspiratory Flow Characteristics. *Journal of International Respiratory Protection* 20:91-101.

Berndtsson, G. 2004. Peak Inhalation Air Flow and Minute Volumes Measured in a Bicycle Ergometer Tests. *Journal of ISRP* 21:21-30.

Blackie, S., McElvaney, N., and Morrison, N. 1991. Normal Values and Ranges for Ventilation and Breathing Pattern at Maximal Exercise. *Chest* 100:136-142.

Caretti, D., Coyne, K., Johnson, A., Scott, W., and Koh, F. 2001. Work Performance When Breathing Through Different Respirator Inhalation and Exhalation Respiratory Inhalation and Exhalation Resistance During Hard Work. *Journal of Occupational and Environmental Hygiene* 3: 214-224.

Caretti D., and Whitely, J. 1998. Exercise Performance during Inspiratory Resistance Breathing Under Exhaustive Constant Load Work. *Ergonomics* 41: 501-511.

Coyne, K., Caretti, D., Scott, W., Johnson, A., and Koh, F. 2006. Inspiratory Flow

Rates During Hard Work When Breathing Through Different Respirator Inhalation and Exhalation Resistances. *Journal of Occupational and Environmental Hygiene* 3: 490-500.

Deno, N.S., Kamon, E., and Kaiser, D.M. 1981. Physiological Responses to Resistance Breathing during short and prolonged exercise. *American Industrial Hygiene Association Journal* 42: 616-623.

Doeblin, E.O. 1996. *Fourth Edition Measurement Systems Application and Design.* New York: McGraw Hill Inc.

"Fleisch Pneumotacograph." [Online] Available at http://www.phippsbird.com/fleisch2.html (Accessed June 1, 2008)

Goldsmith, J. and Young, A. 1956. A New Type of Flow Resistor for Respiratory Studies. 8:562-564.

Goldstein, R. 1996. *Fluid Mechanics Measurements.* Oxfod: Taylor & Francis.

Hansen, D. 1990. Chapter 14 pg 303 of *The Work Environment.* Volume 1.

Harper, P., Brown, CL., and Becks, J.G. 1991. Respirator Physiology Research: Answers in Search of the Question. *Journal of Occupation Medicine* 33: 38-43.

Hayward, A.T.J. 1979. *Flow meters.* New York: Halsted Press.

Heus R., Den Hartog E., and Kistermaker L. 2004. Influence of Inspiratory Resistance on Performance During Graded Exercise Tests on a Cycle Ergometer. Applied Ergonomics 35:583-590.

Holmer, I. 2007. Minute Volume and Inspiratory Flow Rates During Exhaustive Treadmill Walking Using Respirator. *British Occupational Hygiene Society* 51: 327-335.

Holmer I., and Kuklane K. 2002. Respiratory Flow Patterns During Physical Work with Respirators. *National Institute for Working Life Research Report* 2002:12.

Janssen L., Anderson N., Cassidy, P. et al. 2005. Interpretation of Inhalation Airflow Measurements for Respirator Design and Testing. *Journal of the International Society for Respiratory Protection* 22:122-141.

Johnson, A.T., and Cummings, E.G. 1975. Mask Design Considerations. *American Industrial Hygiene Association Journal* 36:220-228.

Johnson, A.T. 1976. The Energetics of Mask Wear. *American Industrial Hygiene Association Journal* 37(8): 479-488.

Johnson, A.T. 1999. *Biological Process Engineering: An Analogical Approach to Fluid Flow, Heat Transfer, and Mass Transfer Applied to Biological Systems*. New York: John Wiley & Sons, Inc.

Johnson, A.T. 1999. Effect of Respirator Inspiratory Resistance Level on a Constant Load Treadmill Work Performance. *American Industrial Hygiene Association Journal.* 60:474-479.

Johnson, A.T. 2006. Why Peak Flow Matters. *Journal of International Society for Respiratory Protection* 23: 100-110.

Johnson, A.T., and Cummings, E. 1975. Mask Design Considerations. *American Industrial Hygiene Association Journal* 36(3):220-228.

Johnson, A.T., Koh, F.C., et al. 2005. Inhalation Flow Rates During Strenuous Exercise. *Journal of International Society for Respiratory Protection* 22:79-96.

Johnson, A.T., Mackey, K. et al. 2005. Exercise Performance While Wearing a Tight Fitting Powered Air Purifying Respirator with Limited Flow. *Journal of Occupational and Environmental Hygiene* 2:368-373.

Johnson, A.T., Scott, W.H. et al. 1997. Sweat Rate Inside a Full Face Piece Respirator. *American Industrial Hygiene Association Journal* 58:881-894.

Johnson, A.T., Micelli, T.M., and Masitis, C. 1973. Flow Regimes in Protective

Masks. (Technical Report EATR 4712). *Edgewood Arsenal, Md.: Department of the Army, Directorate of Development and Engineering.*

Kaufman, J.W. and Hastings, S. 2005. Respiratory Demand During Rigorous Physical Work in a Chemical Protective Ensemble. *Journal of Occupational and Environmental Hygiene* 2: 98-110.

Larson, K. 1994 Sizing Up Micro-machined Instruments. *Controls* 52.

Liptak, B.G. 1993. *Flow Measurement.* CRC Press

Marieb, E. and Hoehn, K. 2007. *Human Anatomy & Physiology Seventh Edition.* San Francisco: Pearson Benjamin Cummings.

Maxfield, Mary. 1971. The Indirect Measurement of Energy Expenditure in Industrial Situation. *The American Journal of Clinical Nutrition* 24:1126-38.

Miller, M.R., Pedersen, O.F., and Quanjer, P.H. 1998. The Rise and Dwell Time for Peak Expiratory Flow in Patients With and Without Airflow Limitation. *American Journal of Respiratory Critical Care Medicine* 158:23-27.

Miller, M.R., Pedersen, O.F., and Sigsgaard, T. 1997. Spirometry with a Fleisch Pneumotachograph: Upstream Heat Exchanger Replaces Heating Requirements. *Journal of Applied Physiology* 82: 1053-1057.

Miller, R.W., 1983. *Flow Measurement Engineering Handbook.* New York: McGraw Hill Inc.

Miller, R.W., 1996. *Flow Measurement Engineering Handbook Third Edition.* New York: McGraw Hill Inc.

Nikishikawq, T., Kobayashi, T., and Mikami et al. 1993. Intelligent Differential Pressure Transmitter Using a Resonant Single Crystal Silicon Sensor. ISA

Ott, R.L., and Longnecker, M. 2001. *An Introduction to Statistical Methods and Data Analysis.* PacIfic Grove: Duxbury.

Rebar, J., Johnson, A.T., Cohen, E., 2004. Effect of Differing Facial Characteristics on Breathing Resistance Inside a Respirator Mask. *Journal of Occupational and Environmental Hygiene* 1:343-348.

Roca, J et al. 1997. Clinical Exercise Testing with Reference to Lung Disease indication, Standardizations and Interpretation Strategies. *European Respirator Journal* 10:2662-89.

Saati, E. 2004. Dynamic Deadspace in Face Masks Used with Non-Invasive Ventilators: a Lung Model Study. *European Respirator* 129-135.

Silver, L., Davidson, G., Janssen, D., et al. 1971. Analytical Modeling of Respiratory Protective Devices. *American Industrial Hygiene Association Journal 32(12):* 775-785.

Silverman, L., Robert, C.L., George, L., Drinker, K.R., and Carpenter, T.M. 1943. Fundamental Factors in the Design of Protective Respiratory Equipment, Inspiratory Air Flow Measurements on Human Subjects with and without Resistance. OSRD report No.1222 Harvard School of Public Health, Boston MA.

Stocks, J., Sly, P., Tepper, R.S., and Morgan, W.J. Infant Respiratory Testing. Published by John Wiley and Sons, 1996.

Stromberg, N.O., and Gronkvist, M.J. 1999. Improved Accuracy and Extended Flow Range for a Fleisch Pneumotachograph. *Medical and Biological Engineering & Computing Journal* 37: 456-460.

Tirimana, P., Herwaddrden, C. et al. 1996. Evaluation of the Suitability of Weekly Peak Expiratory Flow Rate Measurements in Monitoring Annual Decline in Lung Function Among Patients with Asthma and Chronic Bronchitis. *British Journal of General Practice 46:15-18.*

Upp, E.L. 1993. *Fluid Flow Measurement – A Practical Guide to Accurate Flow Measurement.* Houston: Gulf Publishing Company.

Yamashiro, S.M. and Grodins, F.S. 1971. Optimal Regulation of Respiratory Airflow. *Journal of Applied Physiology* 30:597-602.

Yeh, M.P., Gardner, R.M., Adams, T.D., and Yanowitz, F.G. 1982. Computerized determination of pneumotachometer characteristics using a calibrated syringe . *Journal of Applied Physiology* 53:280-285.

Yeh, M.P., Adams, T.D., Gardner, R.M., and Yanowitz, F.G. 1984. Effect of O2, N2, and CO2 composition on nonlinearity of FPCharacteristics. *Journal of Applied Physiology* 56:1423-1425.

Zock, J. 1981. Linearity and Frequency Response of Fleisch Type Pneumotachometer. *European Journal of Physiology* 391:345-352.